NOAA Technical Memorandum NWS NMC-61

SEMI-IMPLICIT HIGHER ORDER VERSION OF THE SHUMAN-HOVERMALE MODEL

National Meteorological Center
Washington, D. C.
April 1978

noaa NATIONAL OCEANIC AND ATMOSPHERIC ADMINISTRATION / National Weather Service

National Meteorological Center
National Weather Service, National Meterological Center Series

The National Meteorological Center (NMC) of the National Weather Service (NWS) produces weather analyses and forecasts for the Northern Hemisphere. Areal coverage is being expanded to include the entire globe. The Center conducts research and development to improve the accuracy of forecasts, to provide information in the most useful form, and to present data as automatically as practicable.

NOAA Technical Memorandums in the NWS NMC series facilitate rapid dissemination of material of general interest which may be preliminary in nature and which may be published formally elsewhere at a later date. Publications 34 through 37 are in the former series, Weather Bureau Technical Notes (TN), National Meterological Center Technical Memoranda; publications 38 through 48 are in the former series ESSA Technical Memoranda, Weather Bureau Technical Memoranda (WBTM). Beginning with 49, publications are now part of the series, NOAA Technical Memorandums NWS.

Publications listed below are available from the National Technical Information Service (NTIS), U.S. Department of Commerce, Sills Bldg., 5285 Port Royal Road, Springfield, Va. 22161. Prices vary for paper copies; $3.00 microfiche. Order by accession number, when given, in parentheses.

Weather Bureau Technical Notes

TN 22 NMC 34 Tropospheric Heating and Cooling for Selected Days and Locations over the United States During Winter 1960 and Spring 1962. Philip F. Clapp and Francis J. Winninghoff, 1965. (PB-170-584)

TN 30 NMC 35 Saturation Thickness Tables for the Dry Adiabatic, Pseudo-adiabatic, and Standard Atmospheres. Jerrold A. LaRue and Russell J. Younkin, January 1966. (PB-169-382)

TN 37 NMC 36 Summary of Verification of Numerical Operational Tropical Cyclone Forecast Tracks for 1965. March 1966. (PB-170-410)

TN 40 NMC 37 Catalog of 5-Day Mean 700-mb. Height Anomaly Centers 1947-1963 and Suggested Applications. J. F. O'Connor, April 1966. (PB-170-376)

ESSA Technical Memoranda

WBTM NMC 38 A Summary of the First-Guess Fields Used for Operational Analyses. J. E. McDonell, February 1967. (AD-810-279)

WBTM NMC 39 Objective Numerical Prediction Out to Six Days Using the Primitive Equation Model--A Test Case. A. J. Wagner, May 1967. (PB-174-920)

WBTM NMC 40 A Snow Index. R. J. Younkin, June 1967. (PB-175-641)

WBTM NMC 41 Detailed Sounding Analysis and Computer Forecasts of the Lifted Index. John D. Stackpole, August 1967. (PB-175-928)

WBTM NMC 42 On Analysis and Initialization for the Primitive Forecast Equations. Takashi Nitta and John B. Hovermale, October 1967. (PB-176-510)

WBTM NMC 43 The Air Pollution Potential Forecast Program. John D. Stackpole, November 1967. (PB-176-949)

WBTM NMC 44 Northern Hemisphere Cloud Cover for Selected Late Fall Seasons Using TIROS Nephanalyses. Philip F. Clapp, December 1968. (PB-186-392)

WBTM NMC 45 On a Certain Type of Integration Error in Numerical Weather Prediction Models. Hans Okland, September 1969. (PB-187-795)

WBTM NMC 46 Noise Analysis of a Limited-Area Fine-Mesh Prediction Model. Joseph P. Gerrity, Jr., and Ronald D. McPherson, February 1970. (PB-191-188)

WBTM NMC 47 The National Air Pollution Potential Forecast Program. Edward Gross, May 1970. (PB-192-324)

WBTM NMC 48 Recent Studies of Computational Stability. Joseph P. Gerrity, Jr., and Ronald D. McPherson, May 1970. (PB-192-979)

(Continued on inside back cover)

NOAA Technical Memorandum NWS NMC-61

SEMI-IMPLICIT HIGHER ORDER VERSION OF THE SHUMAN-HOVERMALE MODEL

Kenneth A. Campana

Kenneth A. Campana

National Meteorological Center
Washington, D. C.
April 1978

UNITED STATES
DEPARTMENT OF COMMERCE
Juanita M. Kreps, Secretary

NATIONAL OCEANIC AND
ATMOSPHERIC ADMINISTRATION
Richard A. Frank, Administrator

National Weather
Service
George P. Cressman, Director

CONTENTS

FIGURES

SEMI-IMPLICIT HIGHER ORDER VERSION OF THE SHUMAN-HOVERMALE MODEL

Kenneth A. Campana
Development Division
National Meteorological Center, NWS, NOAA
Camp Springs, Md.

ABSTRACT. The atmospheric numerical model developed by Shuman and Hovermale at the National Meteorological Center has been reformulated for semi-implicit integration. Orography, moisture, friction, and diabatic effects have been incorporated into this new model. Higher order horizontal finite differencing is used in the advective terms of the model equations to reduce truncation error. Forecasts have been made for a number of real data cases using a time step up to 45 minutes, and the semi-implicit technique has proven stable to at least 7 days. The model is competitive with the operational model at the National Meteorological Center in terms of both forecast accuracy and computation time efficiency.

1. INTRODUCTION

Semi-implicit integration schemes have been used in atmospheric models for a number of years. The implicit treatment is a time-averaging process and is applied to the terms in the model equations governing the fastest moving gravity waves. This acts to slow down these waves and permits a much longer time step to be used than is allowed in a fully explicit model. The computation time savings associated with the longer time step makes the semi-implicit method attractive for atmospheric models being used in operational forecasting environments.

The Shuman-Hovermale (1968) six-layer primitive equation model (6L PE) has been used as an operational forecasting tool for several years at the National Meteorological Center (NMC). With the economic potential of the semi-implicit technique in mind, NMC began to experiment with the 6L PE using this integration scheme. Formulation of the semi-implicit version of the Shuman-Hovermale model was made by Gerrity, McPherson, and Scolnik (1973) and early testing with real data was reported by Campana (1974). The early experiments were feasibility studies conducted with a simplified research model patterned after the 6L PE, but using none of its physical parameterizations and having twice its grid spacing. Since that time, a great deal of effort has been expended in constructing a version of the semi-implicit model which contains all the features of the 6L PE.

The purpose of this report is to document the additions and changes made to the original semi-implicit research model in order to bring it to its new state. No attempt is made to reproduce the multitude of equations and fine details found in the papers of Gerrity et al. (1973) and Campana (1974). Some of the model changes involve only computer programming techniques and are noted here simply for information purposes. A device that allows one to use "variables" rather than numbers in FORTRAN dimension statements makes it easy to change array, and thus grid, sizes. Modular programming, using many small subroutines, simplifies experimentation with various forms of the physical parameterizations. Higher order horizontal finite differencing is feasible because the required number of data rows are always in central memory of the computer. Finally, the ability to switch the model from a semi-implicit mode to an explicit one, which was part of the earlier research model, has been retained.

The details of the NMC semi-implicit model, which have not been discussed elsewhere, will be described in the following sections. Section 2 contains a description of the current method used to obtain initial data for the model. Section 3 discusses the addition of the 6L PE physical processes to the model, but will primarily concentrate on the moisture equation. Section 4 shows the techniques employed to produce stable forecasts beyond the 2-day range. Section 5 describes the higher-order finite differencing on advection processes in the model. Finally, in section 6, some experimental forecasts are presented.

2. INITIAL DATA

Model variables are located on a forecast grid having the same horizontal[1] and vertical resolution as the 6L PE. However, by horizontally staggering the wind components (u,v) with respect to the other model variables (fig. 1), the effective grid mesh length is reduced. In fig. 2 the vertical dimension is shown--p is pressure, T is absolute temperature, $\vec{v}$ is the vector wind, ϕ is geopotential, q is specific humidity, and $\dot{\sigma}$ is vertical motion. The model's vertical structure is a σ system composed of four domains (σ_θ, σ_S, σ_T, σ_B), each of which varies between zero and unity. The history variables are the pressure thickness of each σ-domain, and the temperature, wind, and specific humidity defined at the midpoint of each σ-layer (specific humidity only in the lowest four layers). Diagnostic variables such as ϕ and $\dot{\sigma}$ are defined at the interfaces between σ-layers. In fig. 2, p_θ is the pressure thickness of the computational cap (k=1), p_S is the pressure thickness of the stratosphere (k=2,3), and p_T is the pressure thickness of the troposphere (k=4,5,6,7). The boundary layer (k=7) pressure thickness, p_C, is a constant 50 mbs.

---

[1] 381 kilometers at 60°N on a polar stereographic map projection.

Initial data for the model is obtained from the NMC analyses by using the current 6L PE procedure. Winds in σ layers are obtained from a vertical interpolation of the NMC constant pressure wind analyses rather than the Balance Equation, but otherwise the technique is as described by Shuman and Hovermale (1968). Problems arise when deriving temperatures for the semi-implicit model via this 6L PE initialization scheme, because absolute temperature (T), rather than potential temperature (θ), is the forecast variable. The 6L PE hydrostatic equation is

$$\frac{\partial \phi}{\partial \pi} = - c_p \theta, \tag{1}$$

while for the semi-implicit model it is

$$\frac{\partial \phi}{\partial p} = - \alpha, \tag{2}$$

where the specific volume $\alpha = (RT/p)$; π is the Exner function, $(p/1000)^{R/c_p}$; R is the gas constant; and c_p is the specific heat at constant pressure (the geopotential (ϕ) is defined at σ-interfaces). Eqn. (2) is rewritten as

$$\frac{\partial \phi}{\partial (\ell n\ p)} = - RT \tag{3}$$

or using

$$T = \pi\theta \tag{4}$$

it becomes

$$\frac{\partial \phi}{\partial (\ell n\ p)} = - R\pi\theta, \tag{5}$$

where π is the Exner function defined in σ-layers. Both models should have the same initial distribution of pressure and geopotential (and thus temperature), but θ solutions to the finite-difference forms of eqns. (1) and (5) will differ markedly in the upper atmosphere above 500 mb. To assure the same thermodynamic structure in both the 6L PE and semi-implicit models, the definition of π in eqns. (4) and (5) is changed. Solving eqns. (1) and (5) for π one obtains (in finite-difference form):

$$\pi = c_p/R \frac{\Delta\pi}{\Delta(\ell n\ p)}, \tag{6}$$

where Δ denotes a vertical difference. Note that π on the right side of eqn. (6) is still the Exner function at σ-interfaces. This new definition of π is then used with eqn. (4) whenever there is any conversion between absolute temperature and potential temperature.

The method used to obtain initial data for the computational cap has also been changed. In the operational 6L PE scheme, a complex procedure is employed which insures an initial balance between the wind and mass fields in this topmost model layer. The initial wind field is one of no motion and the procedure produces a pressure and geopotential distribution which has a zero pressure gradient everywhere:

$$\nabla\phi + c_p\theta_{cap}\nabla\pi = 0 \ . \tag{7}$$

The potential temperature, θ_{cap}, is a constant in both space and time. The computational cap pressure gradient in the semi-implicit model, however, is

$$\nabla\phi + \alpha_{cap}\nabla p_\theta \ . \tag{8}$$

The cap pressure thickness is set to a constant 100 mb at all grid points, thus making the second term in eqn. (8) initially zero. Therefore, to obtain an initial balance between wind and mass fields, one need only look at the geopotential term. Defining α_{cap} to be constant in space and time and using eqn. (2), one sees that the $\nabla\phi$ term is identical at top and bottom of the cap. Since the initial winds at 100 mb are constrained to be in at least geostrophic balance by the NMC analysis scheme, use of these winds as initial data for the cap should result in a balanced state. Thus, for the cap (k = 1 in fig. 2)

$$p_\theta = 100 \text{ mb}$$

$$u_1 = u \text{ at } 100 \text{ mb}$$

$$v_1 = v \text{ at } 100 \text{ mb}.$$

The constant specific volume, α_{cap}, is defined by the Equation of State below:

$$\alpha_{cap} = RT/p$$

where $T = 250^oK$[1] and $p = 50$ mb.

---

[1]A temperature below 200^oK produced a model failure during a forecast while a temperature over 400^oK produced a large temporal oscillation in the model stratosphere.

Several other changes have been made to the 6L PE initialization scheme and they are noted below:

1. The tropopause (σ-interface above layer 4 in fig. 2) is redefined so that its pressure is never less than 200 mb. This insures an initial stratospheric pressure thickness of at least 100 mb. During the forecast cycle this constraint is removed.

2. No initial moisture is available for the topmost tropospheric layer, so none is defined ($q_1 \equiv 0$). Any moisture accumulating there during a forecast comes from vertical advection processes.

3. The NMC wind analyses produce u,v components at grid point locations, whereas the semi-implicit model needs them at grid box locations; (see fig. 1). Wind data are interpolated horizontally from the grid points using a biquadratic scheme--a Bessel interpolation formula with second-order terms (Saucier 1955, p. 121).

4. Orography is now part of the semi-implicit model. Necessary changes to the original method of splitting the orographic terms into implicit and explicit parts have been made by Campana (1978). The 6L PE mountain field is used, but it is filtered horizontally using Shuman's (1957) nine-point smoother. Unfiltered mountains produced model failures in both semi-implicit and explicit versions of the new model after 1½ forecast days. These difficulties were noise problems and were not related to those documented by Campana (1978).

3. MODEL PHYSICS

All physical processes contained in the 6L PE are included in the semi-implicit model. Since they have been discussed by Shuman and Hovermale (1968), fine details are omitted from this report. Modifications are made to the semi-implicit model in order to use existing FORTRAN coded algorithms from the 6L PE model. Absolute temperature is converted to potential temperature, via eqns. (4) and (6), in order to use the existing dry and moist convective adjustment schemes. After the adjustment, the reverse conversion occurs, from θ to T. Eqns. (4) and (6) are also used to obtain long-wave cooling rates for the new model that are equivalent to those of the 6L PE.

The primary purpose of this section is to document the addition of a moisture variable to the semi-implicit model. Specific humidity, q, is used and is defined in the four σ-layers below the model tropopause (fig. 2). In order to use the precipitation, latent heating, and solar absorption (due to moisture) algorithms from the 6L PE, specific humidity is converted temporarily to precipitable water, PWAT:

$$\mathrm{PWAT} = (1/g)\int q\frac{\partial p}{\partial \sigma}\, d\sigma \ , \qquad (9)$$

where g is gravity.

The moisture equation (10) and its finite difference forms are presented below in order to complete the set of model equations given by Gerrity et al. (1973):

$$\frac{\partial q}{\partial t} = - m\left(u\frac{\partial q}{\partial x} + v\frac{\partial q}{\partial y}\right) - \dot{\sigma}\frac{\partial q}{\partial \sigma} + CE\,, \tag{10}$$

where the symbols are:

t = time

x,y = horizontal coordinates

σ = vertical coordinate

u,v = horizontal wind components

$\dot{\sigma}$ = vertical wind component

m = map factor

CE = influence of condensation and evaporation (as in 6L PE)

Since moisture influences the model through latent heating from the precipitation algorithm, which in turn is part of the explicitly calculated terms in the thermodynamic equation, eqn.(10) is completely explicit (i.e., no semi-implicit parts). Initial fears concerning excess precipitation associated with the long time step in the semi-implicit model have proven unfounded.

The most difficult term to compute in eqn. (10) is the vertical advection term, $\dot{\sigma}\ \partial q/\partial\sigma$. The evaluation of this term at the top of the boundary layer is quite complex. A formulation exactly the same as described in Gerrity et al. (1973, section 3.5) is used, where the $\partial q/\partial\sigma$ term at this interface is defined below for both the troposphere (subscript T) and the boundary layer (subscript B).

$$\frac{\partial q}{\partial \sigma_T} = 6\mu^*(q_4 - q_3) \tag{11}$$

$$\frac{\partial q}{\partial \sigma_B} = 2(1 - \mu^*)(q_4 - q_3) \tag{12}$$

$$\mu^* = \frac{p_T - p_c}{p_T + 2p_c} \tag{13}$$

Note that p_T and p_c are the tropospheric and boundary layer pressure thicknesses, respectively; [see Gerrity et al. 1973, eqns. (129) and (130)]. The following equation is useful when discussing the specifics of the moisture equation. It relates the two definitions of $\dot{\sigma}$ at the top of the boundary layer which are valid either in the troposphere ($\dot{\sigma}_7$) or in the boundary layer ($\dot{\sigma}_B$)--see eqn. (134) Gerrity et al. (1973):

$$\dot{\sigma}_B = \frac{p_T - p_c}{p_c} \dot{\sigma}_7 \tag{14}$$

The moisture equation in the troposphere ($k = 1,2,3$ for q) becomes

$$\frac{\partial q_k}{\partial t} = - m\left\{u_{k+3} \frac{\partial q_k}{\partial x} + v_{k+3} \frac{\partial q_k}{\partial y}\right\} - M_k + CE \tag{15}$$

$$M_1 = 3/2\ \dot{\sigma}_5 (q_2 - q_1) \tag{16}$$

$$M_2 = M_1 + 3/2\ \dot{\sigma}_6 (q_3 - q_2) \tag{17}$$

$$M_3 = M_2 - M_1 + 6\ \mu^*/2\left(\dot{\sigma}_7 (q_4 - q_3)\right) \tag{18}$$

Since the vertical advection, $\dot{\sigma}\ \partial q/\partial\sigma$, is computed <u>at</u> σ-interfaces, the "½" in the M_k term comes from vertically averaging $\dot{\sigma}\ \partial q/\partial\sigma$ to the σ-layers.

In the boundary layer ($k = 4$ for q), eqn. (10) is:

$$\frac{\partial q_4}{\partial t} = - m\left(u_7 \frac{\partial q_4}{\partial x} + v_7 \frac{\partial q_4}{\partial y}\right) - M_4 + CE \tag{19}$$

$$M_4 = \tfrac{1}{2}\ \dot{\sigma}_B \mu_B (q_4 - q_3) \tag{20}$$

where $\dot{\sigma}_B$ is defined in eqn. (14) and

$$\mu_B = 2(1 - \mu^*) \tag{21}$$

The finite difference forms of the horizontal and vertical advection terms in eqns. (15) and (19) are consistent with the other model equations. The reader's attention is drawn to Shuman and Hovermale (1968) where the finite-difference notation used below is defined. Noting that overbars, $\overline{(\ )}^x$, $\overline{(\ )}^y$, refer to averaging processes along

specified grid axes, representative terms are calculated as follows:

$$u\frac{\partial q}{\partial x} + v\frac{\partial q}{\partial y} \rightarrow \overline{u\,\overline{q}_x^{\,y} + v\,\overline{q}_y^{\,x}}^{\,xy} \tag{22}$$

$$M_1 \rightarrow 3/2\,\overline{\dot{\sigma}_5^{\,xy}\,\overline{(q_2 - q_1)}^{\,xy}}^{\,xy} \tag{23}$$

Careful consideration of where each variable is located on the grid shows that the above finite differences are valid at the same locations as q.

4. MODEL STABILITY

Techniques used to control computational noise that develops during a 6L PE forecast are also included in the semi-implicit model. They are quite effective in damping noise and allowing the forecast to proceed reliably beyond 48 hours.

The first tool employed is a time filter of the form used by Asselin (1972) which controls high frequency noise developing during a model forecast. The filter is shown in eqn. (24) and is applied at each time step to the u and v wind components.

$$(\,)^* = \xi(\,)^{\tau} + \frac{1-\xi}{2}\left[(\,)^{\tau+1} + (\,)^{*\tau-1}\right], \tag{24}$$

where $\xi = 0.3$ and $\tau-1, \tau, \tau+1$ superscripts refer to past, present, and future time levels. After obtaining $\tau+1$ variables, eqn. (24) is solved for the time filtered variable, $(\,)^*$. This new quantity is used during the succeeding forecast cycle when it becomes the $\tau-1$ variable. Limited testing with a larger ξ, meaning less filtering, allowed too much computational noise to develop in the wind fields.

The second technique controls high wave number noise in space. It is a Shuman (1957) smoother-desmoother and is applied to pressure, temperature, and moisture variables at each time step. These spatially smoothed quantities become the $\tau-1$ variables in the succeeding forecast step. In the 6L PE it is applied to only pressure and temperature; the smoothing coefficient, ν, has a value of .022 with a 10-minute step. Noting that the strength of the filter depends on the number of times that it is applied, as well as the size of ν, the semi-implicit model coefficient is approximately 2½ times stronger than that used in the 6L PE.[1]

---

[1]The coefficient, ν, would be equivalent to 0.058 in the 6L PE.

An experiment with a filter half as strong, and thus similar to the 6L PE, produced results in which meteorological features differed little from the heavier filter test. At 48 hours, the 500-mb height forecasts are virtually identical (figs. 3 and 4). By 84 hours, however, there are some small differences in the intensity of meteorological features, but more importantly, computational noise appears in the weaker filter test (figs. 5 and 6). Thus, the heavier smoother is beneficial to the model without adversely affecting its forecasts of meteorological scale features.

Another device is used to control problems in the model stratosphere. The semi-implicit model constrains the stratosphere to be at least 50 mb thick during a forecast by "adding mass" from the model troposphere at offending grid points. Whenever this occurs the wind field has become noisy, so the winds are mixed vertically and horizontally. Noting that the u,v wind components are staggered with respect to the other variables, the four u,v winds surrounding the offending stratospheric pressure are averaged to the grid point and mixed vertically as in the 6L PE. The vertically mixed wind is inserted back into the four surrounding u,v locations in each σ-layer which participated in the vertical mixing. The 6L PE uses 6 mb as its limiting pressure thickness, but by the time the stratosphere has become that thin, all other variables must be rather nonmeteorological. Reflecting the stability of the semi-implicit model, this stratospheric device is rarely needed during a forecast.

Both the time and space filters act to reduce the maximum allowable time step of the model, but they have helped create a stable forecast model.[1] In the only attempt at "long-range" forecasting with the semi-implicit model, forecasts were made out to 168 hours from 0000 GMT 17 February 1977. Although necessarily smooth, the large-scale meteorological features appear quite realistic (fig. 7). No verification is presented for this forecast, however.

5. HIGHER ORDER FINITE DIFFERENCING

Although not related to the semi-implicit method, higher order (horizontal) finite differencing has been quite successful in the new model. Thus it is deemed to be of sufficient interest to be included in this report. Its use in the model is based on the paper by Gerrity, McPherson, and Polger (1972). There the conclusion was that higher order, more accurate, forms of Shuman's (1968) semimomentum finite-differencing for the advective processes would reduce truncation error in a grid point model while requiring only a slight decrease in time step length. The reduction in truncation error would result in

---

[1]A backward implicit time differencing technique used in conjunction with the time filter is an alternative method for controlling non-meteorological noise in the model. Little experimentation has been done with this technique.

improved translation speeds of meteorological-scale features. Often the major difference between the 6L PE and its finer mesh counterpart, the LFM[1], is the speed with which major features are moved during a forecast--the LFM being more accurate. Higher order differencing could make the 6L PE more competitive with the LFM in these cases. Of course, in situations where the resolution of the finer mesh is necessary to delineate important small-scale features in the initial data and during the forecast, the LFM probably will be superior.

A paper by Gerrity (1973) shows the higher-order scheme that is used with the semi-implicit model. These fourth-order[2] differences are applied to the advective terms in all model equations; although near model boundaries, where fewer grid points are available, second-order approximations are used. The derivation of the higher-order finite-difference forms is not presented here; however, Gerrity's (1973) eqns. (14) and (15) are shown below. Fourth-order averaging in one dimension is

$$\overline{(\,)}^{x_h} \equiv 9/8\overline{(\,)}^{x} - 1/8\overline{(\,)}^{3x} , \tag{25}$$

while fourth-order differencing is

$$(\,)_{x_h} \equiv 9/8(\,)_x - 1/8(\,)_{3x} , \tag{26}$$

where $\overline{(\,)}^{x}$, $(\,)_x$ are Shuman's regular second-order approximations and $\overline{(\,)}^{3x}$, $(\,)_{3x}$ are derived from them.

The fourth-order semi-implicit model's finite difference form for the advection terms are shown below. Eqn. (22) from section 3 becomes

$$u\frac{\partial q}{\partial x} + v\frac{\partial q}{\partial y} \rightarrow \overline{\left(u\,\overline{q}^{y_h}_{x_h} + v\,\overline{q}^{x_h}_{y_h}\right)}^{x_h y_h} . \tag{27}$$

The advection terms in the equations of motion are handled somewhat differently due to the staggering of variables

$$u\frac{\partial u}{\partial x} + v\frac{\partial u}{\partial y} \rightarrow \overline{\left(\overline{u}^{xy}\,\overline{u}^{y_h}_{x_h} + \overline{v}^{xy}\,\overline{u}^{x_h}_{y_h}\right)}^{x_h y_h} . \tag{28}$$

---

[1]Limited-area fine-mesh model--grid distance of 190.5 km at 60°N on a polar stereographic map projection.

[2]The order of the scheme refers to the exponential power of the grid interval in the leading term of those omitted from a series expansion of the finite-difference form--the higher the order, the more terms are retained.

Note that the advecting wind in eqn. (28) contains second-order averaging. Although all results documented in this report use this second-order approximation on the advecting wind, a fourth-order form is more consistent with the finite differencing.[1] For future testing of this model, changes have been made that use fourth-order averaging on the advecting wind.

6. RESULTS

A number of experiments have been made using the semi-implicit version of the Shuman-Hovermale model at NMC. Some of the results from six case studies made from initial data for October 1976 are presented in this section. Pressure level data for the semi-implicit model are interpolated from σ data in exactly the same manner as for the 6L PE. This has necessitated an averaging of the u,v winds to the grid points and a resultant small loss in amplitude for any quantity derived from these velocity fields. In order to keep the various versions of the new model from confusing the reader, the following abbreviations are defined:

S4 - semi-implicit, fourth-order finite differencing
S2 - semi-implicit, second-order finite differencing
E4 - explicit version, fourth-order finite differencing
E2 - explicit version, second-order finite differencing

The main advantage of the semi-implicit method is the longer time step permitted and the associated savings in computation time. This saving is partially offset by having to solve a set of Helmholtz equations for each time step. Using an iterative process described by Sela and Scolnik (1972), these equations are transformed so that each one can be solved independently by a two-dimensional Liebmann relaxation scheme. When using this method on the IBM 360/195 system, double precision arithmetic (64-bit word) is required for the transformation process and the relaxation scheme. Each independent equation provides one of the model's pressure thicknesses (p_θ, p_S, p_T) or one of the non-zero vertical motions ($\dot{\sigma}$). Each equation has a separate over-relaxation coefficient in order to speed up the computations. The convergence criteria are for the transformed variables and translate into approximately 10^{-2} mb for the pressure thicknesses and 10^{-9} mb/sec for $\dot{\sigma}$. In practice, the relaxation calculations account for about 10% of the total computation time (the transformation process takes an additional 5%).

---

[1] Several comparisons of 48-hr forecasts made using second or fourth-order averaging showed little difference.

No experiments have been made to determine the maximum allowable time step for either the S2 or S4 models, but the S2 model has safely used a 45-minute step. During about half the calendar year, a 45-minute step has been used with the S4 model; however, in winter months when the wind speeds are higher a shorter step is needed. For convenience, 30 minutes is used. Table 1 shows some approximate computation times for 48-hour forecasts using different versions of the new model. This does not include the "wait" time involved with reading from or writing to disk.

Table 1. Approximate computation times for 48-hour forecasts.

Time Step	Model	Time for 48-hr Forecast (min)
45	S2	9.25
45	S4	10.00
30	S4	13.75
7.5	E4	36.00

Note from the first two entries in the table that the more complex calculations used in the higher order finite differences for the S4 model increase the computation time by about 10%. Comparing the E4 model with its time step of 7.5 minutes and the S4 model with a time step of 45 minutes, there is almost a 4:1 ratio in computation time. If the more expensive radiation calculations were made every time step in the E4 model, as is done in the S4 model, then a 4:1 ratio would easily be attained.

Since the higher order finite difference scheme is chosen to be used with the semi-implicit model, it is instructive to show some results that led to this decision. Sea level pressure and 500-mb height forecasts for 24 and 48 hours are shown in figs. 8 to 15. The comparisons are between the E2 model and the more accurate E4 model for a case (0000 GMT October 8, 1976) in which the 6L PE produced a poor 48-hour forecast over North America. At 24 hours (figs. 8 to 11), there is little difference between the E2 and E4 models; however, by 48 hours (figs. 12 to 15) the fourth-order scheme has resulted in faster motion for the meteorological features primarily at 500 mb. The faster movement of the ridge-trough pattern over the United States at 48 hours verifies better against the analysis (fig. 27) than the E2 model forecast. While other test cases are not described in this report, indications from them are that the faster translational speeds due to the higher order scheme are more pronounced at higher atmospheric levels where wind speeds are stronger.

It seems that in every paper on the semi-implicit method in the literature, the point is made that there is little difference between explicit and semi-implicit versions of the same model. In keeping with

tradition, this author will do likewise. Comparison is made between the fourth-order models S4 and E4 for the October 8, 1976 case. Figures 13 and 22 show 48-hour forecasts of sea level pressure; figs. 15 and 25 show 500-mb height forecasts; and figs. 28 and 29 show 36-48 hour accumulated precipitation (centimeters) for the E4 and S4 models, respectively. The explicit version is somewhat noisier in the tropical regions and its stronger vertical motion probably accounts for the precipitation differences, but overall the forecasts for the two models are virtually identical. This is brought out more dramatically in fig. 31. It is a graph of S1 scores at 500 mb for the six test cases in October 1976. Twenty-four and 48-hour scores in three NMC verification areas over the Northern Hemisphere are shown. Each point on the graph gives the appropriate S1 score for the E4 (abscissa) and S4 (ordinate) models. The models are equivalent in S1 score if the points fall on the 45° diagonal. As can be seen, the models are virtually identical at 500 mb for both forecast hours.

One might speculate how the new model compares with the 6L PE. Since the 6L PE has second-order finite differencing, the fairest comparison is with the E2 model. However, one should expect some difference simply because the effective grid length of the E2 model is smaller due to the staggering of forecast variables. The time step for the E2 model is only 7.5 minutes compared with 10 minutes for the 6L PE. Differences in orography, initial winds, and smoothing coefficients will also contribute to differences in the results. Forecasts for the October 8 case are shown in figs. 8, 10, 12, and 14 for the E2 model and in figs. 17, 20, 23, and 26 for the 6L PE. The reader will be able to make more comparisons than will be put into this report, but several conclusions may be drawn. First, the E2 forecasts appear smoother than the 6L PE--compare 24-hour sea level forecasts in the Gulf of Alaska in figs. 8 and 17. Second, at 48 hours the E2 forecasts have moved some features faster (and more correctly) than the 6L PE--compare the sea-level low pressure north of the Caspian Sea in figs. 12 and 23, and compare the lower part of the 500-mb trough over southeastern United States in figs. 14 and 26. Model comparisons using graphs of S1 scores at sea level and 500 mb are shown in figs. 32 and 33. At sea level there may be a slight advantage given to the E2 model by 48 hours; however, at 500 mb the E2 model is clearly superior to the 6L PE. These results may be due, in part, to the smoother E2 forecasts.

The most competitive model with respect to the 6L PE is the S4 version--both in terms of computational speed (semi-implicit) and in terms of accuracy (fourth-order differencing). Forecasts for the S4 model are shown in figs. 16, 19, 22, and 25, and they can be compared with those of the 6L PE (figs. 17, 20, 23, and 26) or the E2 model (figs. 8, 10, 12, and 14). Verification charts are shown in figs. 18, 21, 24, and 27, while the 12-hour accumulated precipitation for the 36- to 48-hour period

is shown in fig. 29 for the S4 model and in fig. 30 for the 6L PE. The same conclusions can be drawn about the comparison between the two models as was done above for the E2 model. The S4 forecasts appear smoother than those of the 6L PE, and translation speeds of meteorological systems are faster. The potential for better numerical forecasts using a more accurate higher order scheme is shown in the 48-hour 500-mb map over the eastern United States (compare figs. 25 and 26 with fig. 27). While some of this good forecast can be attributed to the new model (E2 shows improvement over the 6L PE), much of it results from the higher order scheme (compare fig. 25 with fig. 14). Graphs of S1 scores for the S4 model and the 6L PE are shown in figs. 34 and 35. While at sea level there is no clear victor, the S4 model is superior at 500 mb in most instances.

7. CONCLUSIONS

The Shuman-Hovermale numerical model at NMC has been reformulated successfully for semi-implicit time integration. Tests have been made with various versions of the new model and comparisons have been made using forecast results. Several conclusions are noted below:

1) Semi-implicit and explicit versions of the new model produce virtually identical forecasts. The vertical motion in the semi-implicit tests has less amplitude than in the explicit runs and this appears as less noise on pressure level maps. This does not make the comparable forecasts any less identical.

2) The new model in its second-order form is superior to the 6L PE. Since both models have virtually the same initial data and produce pressure level forecast maps in an identical manner, the superiority of the new model seems due its reduction of effective grid length by staggering variables horizontally. However, there may be some loss of detail in the new model due to the heavier smoothing.

3) Higher-order finite differencing on the horizontal advection terms in the model has increased the translation speeds of some meteorological-scale features--usually in a more correct sense. The effect seems more pronounced at higher atmospheric levels where wind speeds are stronger, and at longer forecast times when the cumulative effect of the greater accuracy becomes more apparent.

No plans have been made to use the new model as an operational tool, even though it produces forecasts that are generally superior to those of the 6L PE. It requires about the same amount of computer resources as the operational model, because it uses the same horizontal grid mesh; however, its computation efficiency is not impressive when compared with the highly optimized 6L PE. Of course, the semi-implicit

version of the new model is quite efficient when compared with its explicit counterpart (table 1), but the crucial computation time in the NMC operational environment is the one which includes "wait" time associated with input/output operations. This "wall" time is approximately 24 minutes for a 48-hour 6L PE forecast. Some work has been done to optimize the new model, but the best wall times for the semi-implicit versions are approximately twice those times listed in table 1--that is, about 19 minutes for the S2 model and about 28 minutes for the S4 model (30-minute time step). The question of computational efficiency (i.e., wall time) will need to be resolved if the new model is to become useful operationally. If the S4 model with its more accurate finite differencing produces forecasts that are competitive with the finer mesh version of the 6L PE currently being tested,[1] then this question of efficiency recedes into the background.

ACKNOWLEDGMENTS

The author wishes to thank Joseph Gerrity for his important contribution toward incorporating orography into the model; also Bill Collins for his much needed assistance in obtaining initial temperature data in the model that is equivalent to the 6L PE. Finally, special thanks to Mary Daigle for typing the report, to Bob van Haaren for producing the S1 scores, and to Tom Krzenski for drafting some of the figures.

---

[1]Wall time over an hour for a 48-hour forecast.

REFERENCES

Asselin, Richard A., "Frequency filter for time integrations," Monthly Weather Review, 100, 1972, pp. 487-490.

Campana, Kenneth A., "Status report on a semi-implicit version of the Shuman-Hovermale model," NOAA Technical Memorandum NWS-NMC 54, 1974, 22 pp.

Campana, Kenneth A., "Addition of orography to the semi-implicit version of the Shuman-Hovermale model," to be published as a NOAA Technical Memorandum in 1978.

Gerrity, Joseph P., McPherson, Ronald D., and Polger, Paul D., "On the efficient reduction of truncation error in numerical weather prediction models," Monthly Weather Review, 100, 1972, pp. 637-643.

Gerrity, Joseph P., "Numerical advection experiments with higher order, accurate, semi-momentum approximations," Monthly Weather Review, 101, 1973, pp. 231-234.

Gerrity, Joseph P., McPherson, Ronald D., and Scolnik, Stephen, "A semi-implicit version of the Shuman-Hovermale model," NOAA Technical Memorandum NWS-NMC 53, 1973, 44 pp.

Saucier, Walter J., Principles of meteorological analysis, University of Chicago Press, 1955, 438 pp.

Sela, Joseph, and Scolnik, Stephen, "Method for solving simultaneous Helmholtz equations," Monthly Weather Review, 100, 1972, pp. 644-645.

Shuman, Frederick G., "Numerical methods in weather prediction, II. Smoothing and filtering," Monthly Weather Review, 85, 1957, pp. 357-361.

Shuman, Frederick G., and Hovermale, John B., "An operational six-layer primitive equation model," Journal of Applied Meteorology, 7, 1968, pp. 525-547.

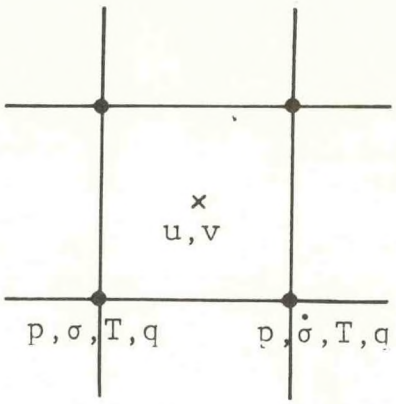

Figure 1.--Location of forecast variables on the horizontal grid.

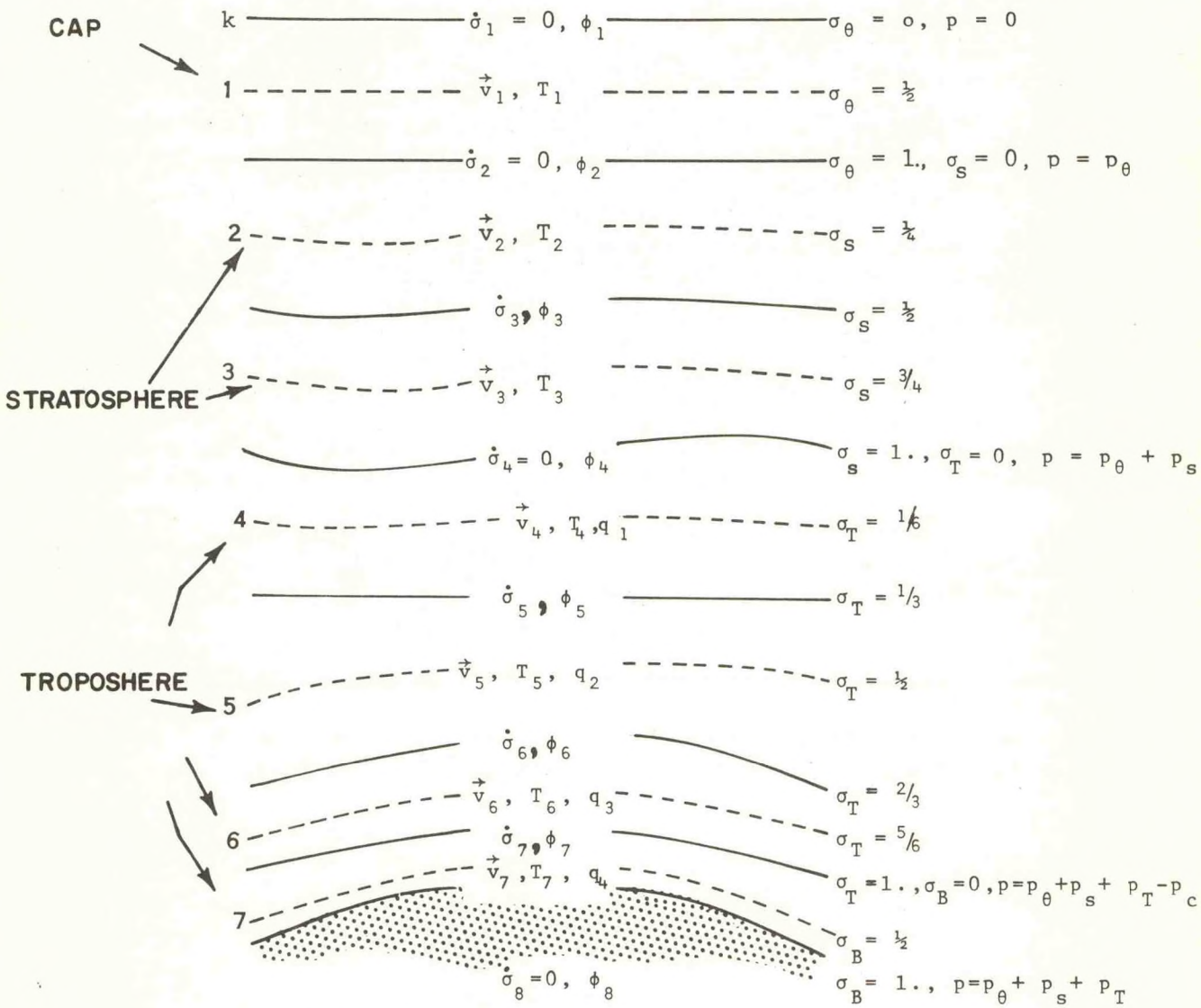

Figure 2.--Vertical structure of the model.

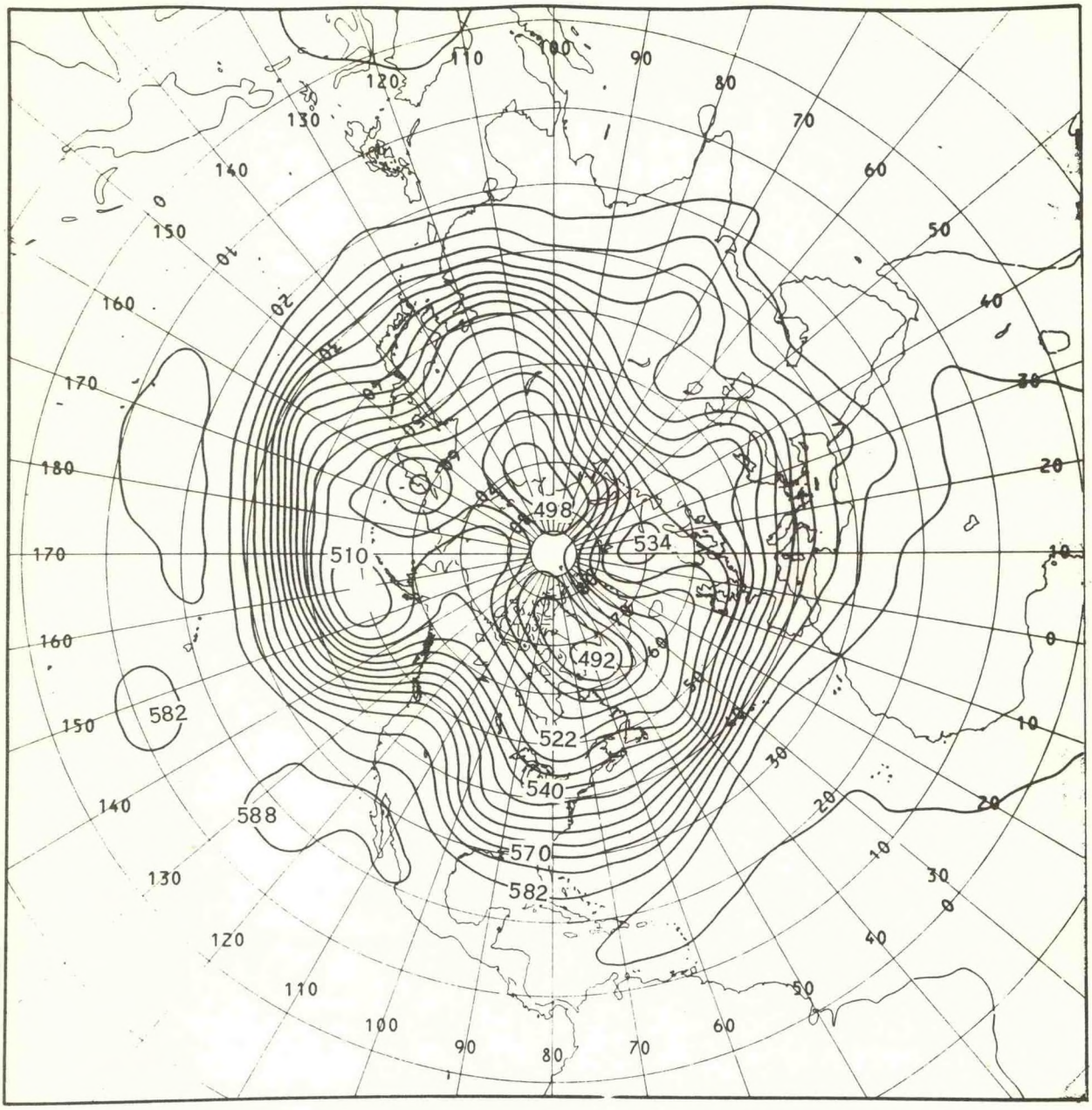

Figure 3.--Semi-implicit 500-mb heights, 48 hr from 0000 GMT Feb. 17, 1977, with regular smoothing--contour interval 6 decameters.

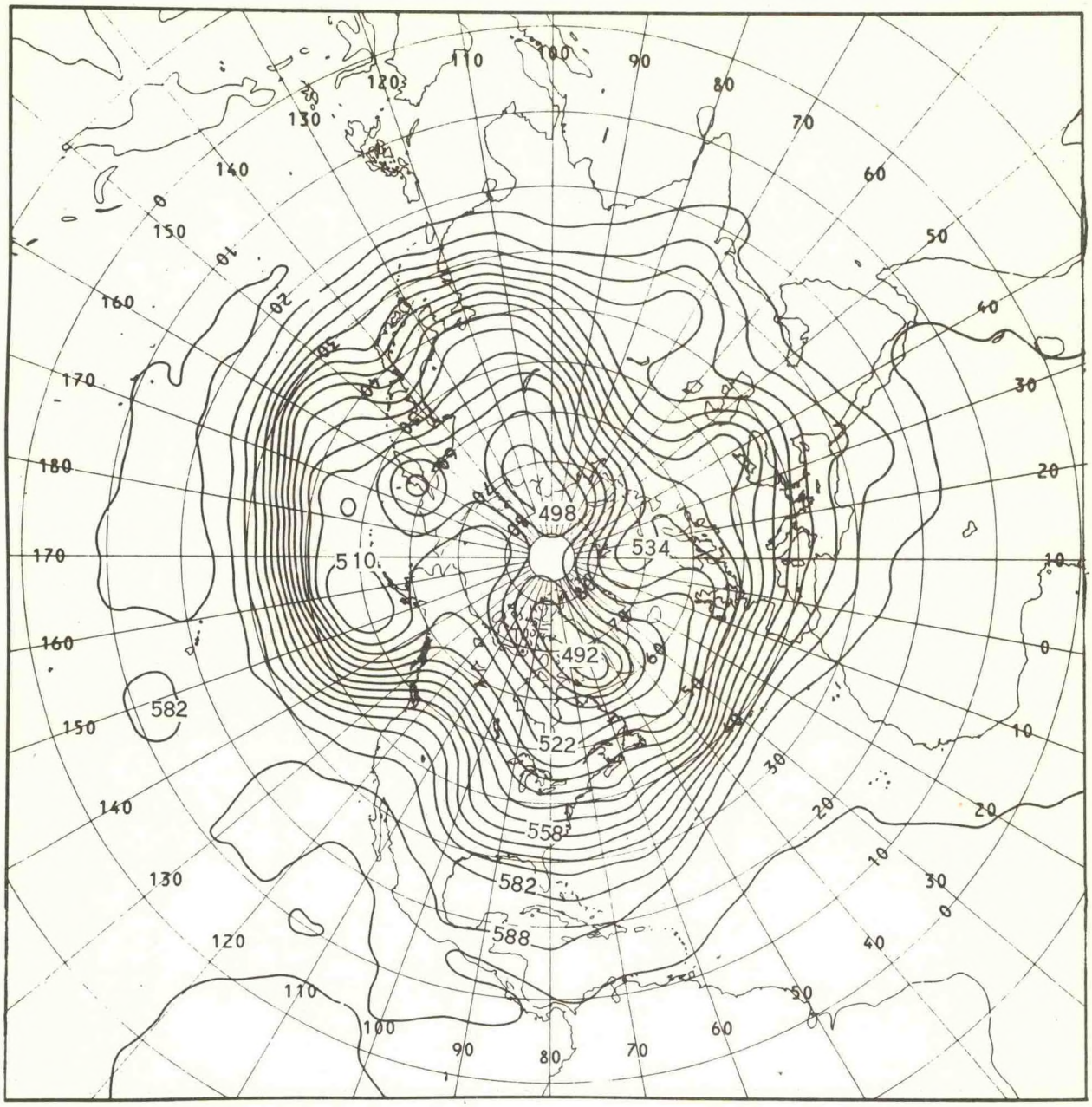

Figure 4.--Semi-implicit 500-mb heights, 48 hr from 0000 GMT Feb. 17, 1977, with one-half the regular smoothing--contour interval 6 decameters.

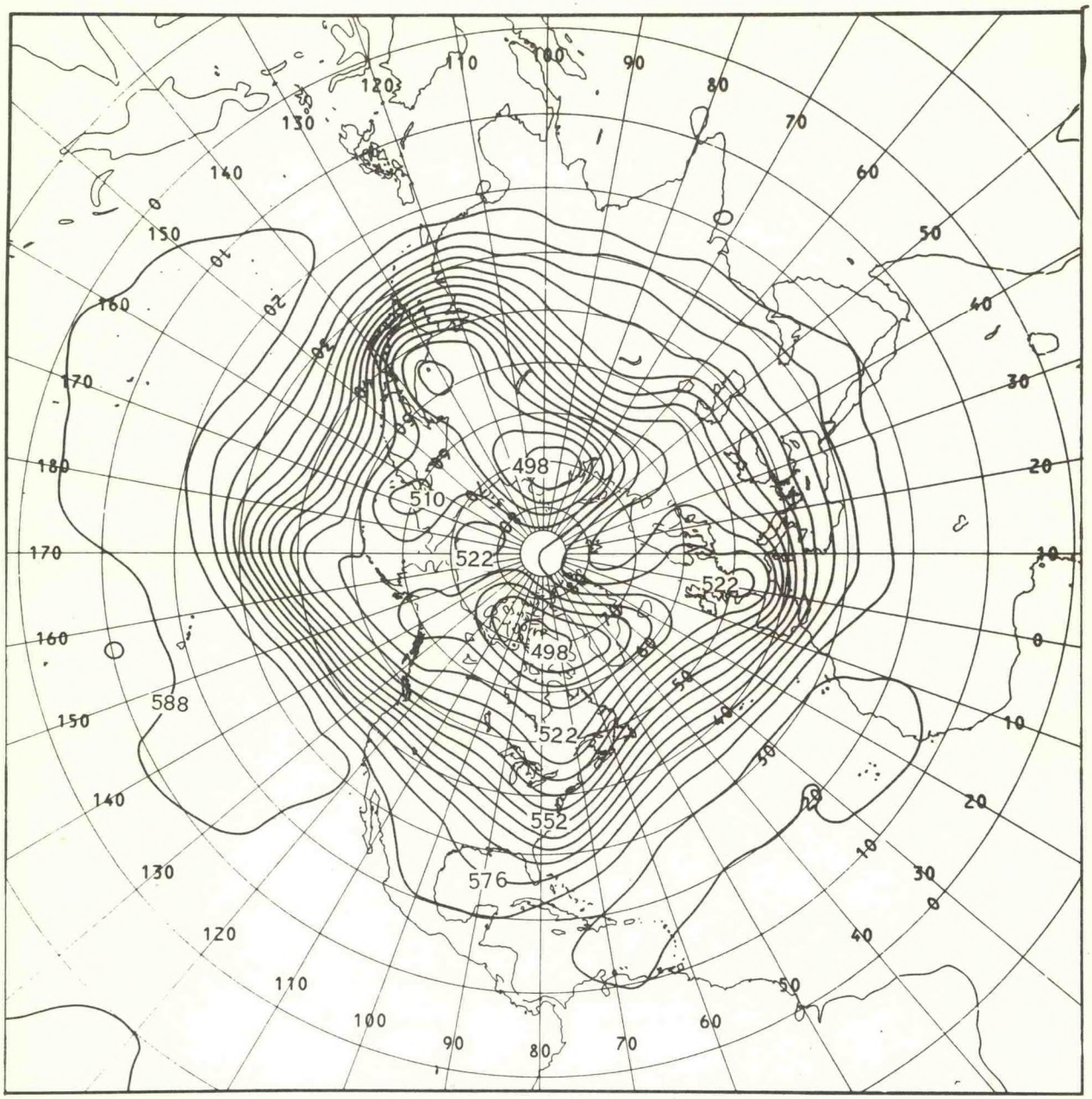

Figure 5.--Semi-implicit 500-mb heights, 84 hr from 0000 GMT Feb. 17, 1977, with regular smoothing--contour interval 6 decameters.

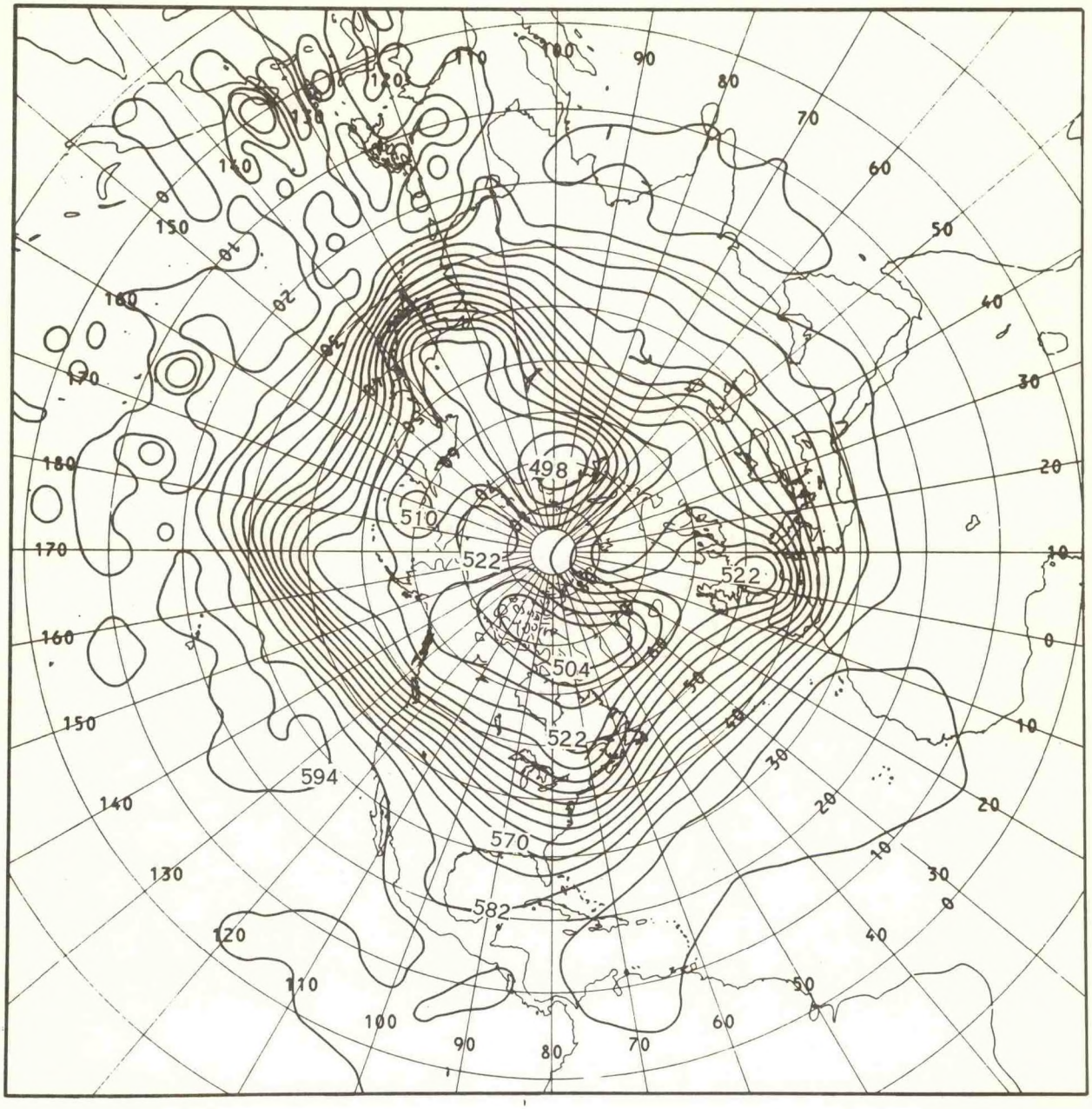

Figure 6.--Semi-implicit 500-mb heights, 84 hr from 0000 GMT Feb. 17, 1977, with one-half the regular smoothing--contour interval 6 decameters.

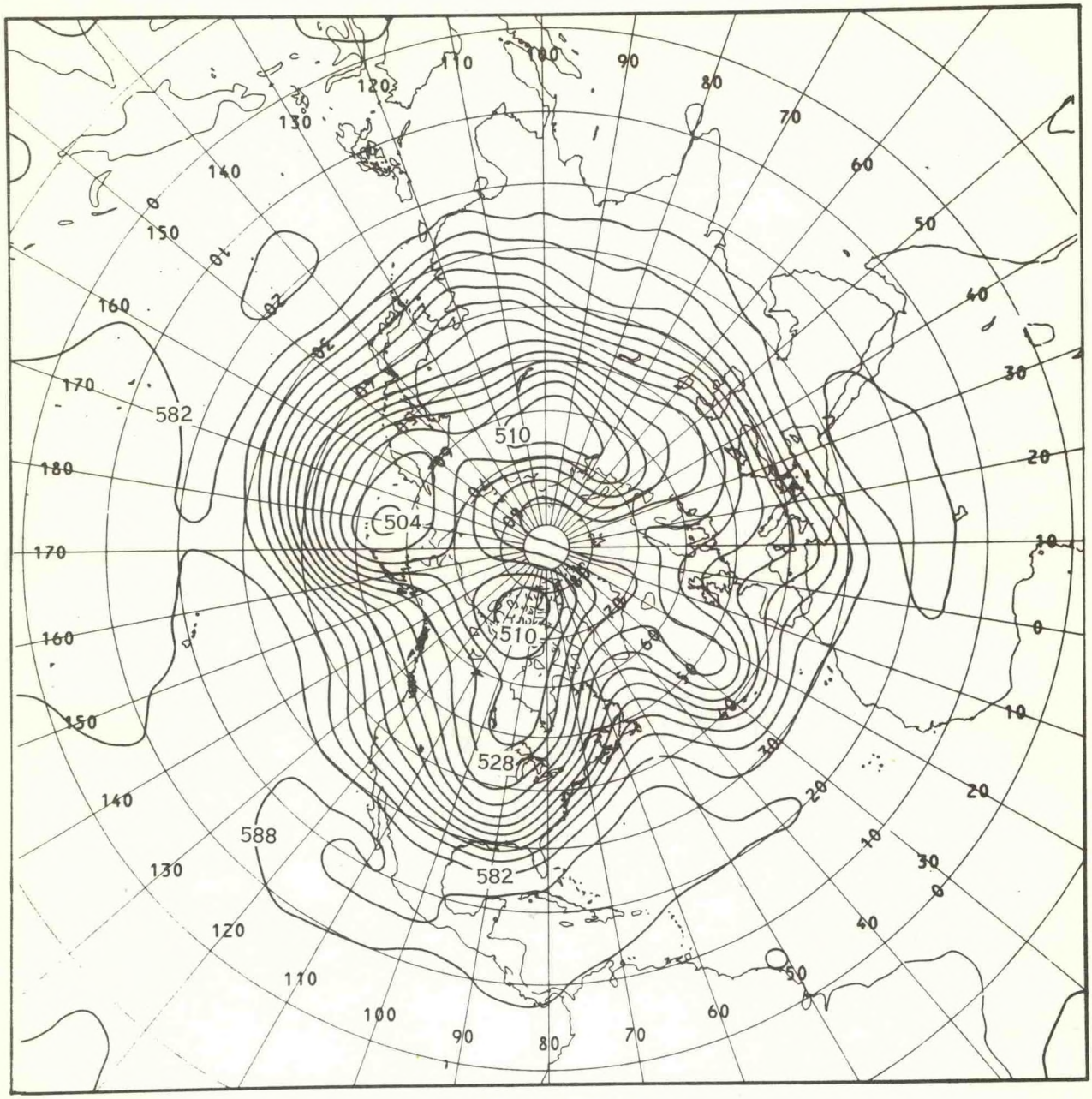

Figure 7.--Semi-implicit, fourth order, 500-mb heights, 168 hr from 0000 GMT Feb. 17, 1977-- contour interval 6 decameters.

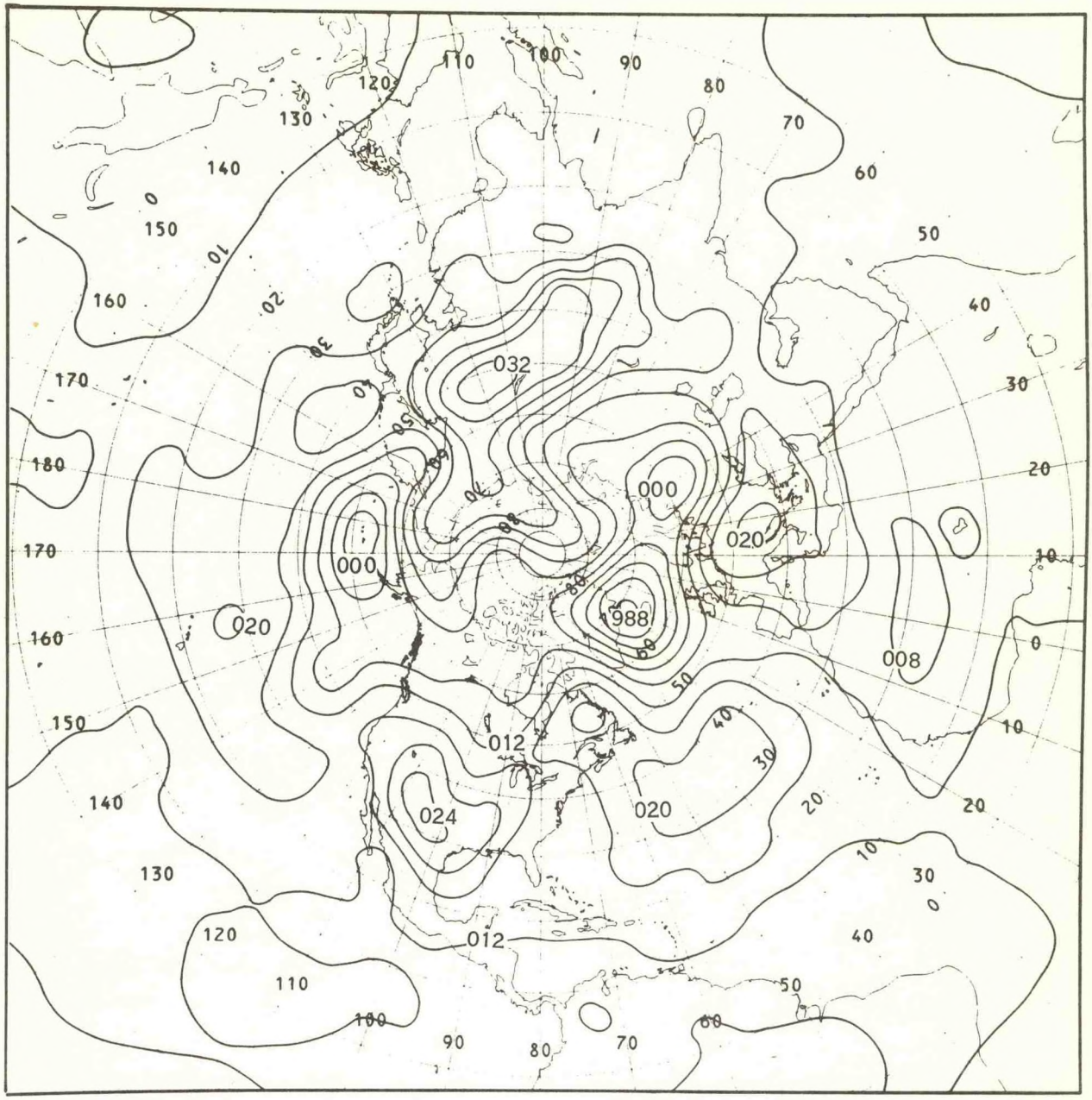

Figure 8.--E2 model, sea level pressure, 24 hr from 0000 GMT Oct. 8, 1976--contour interval 4 mb.

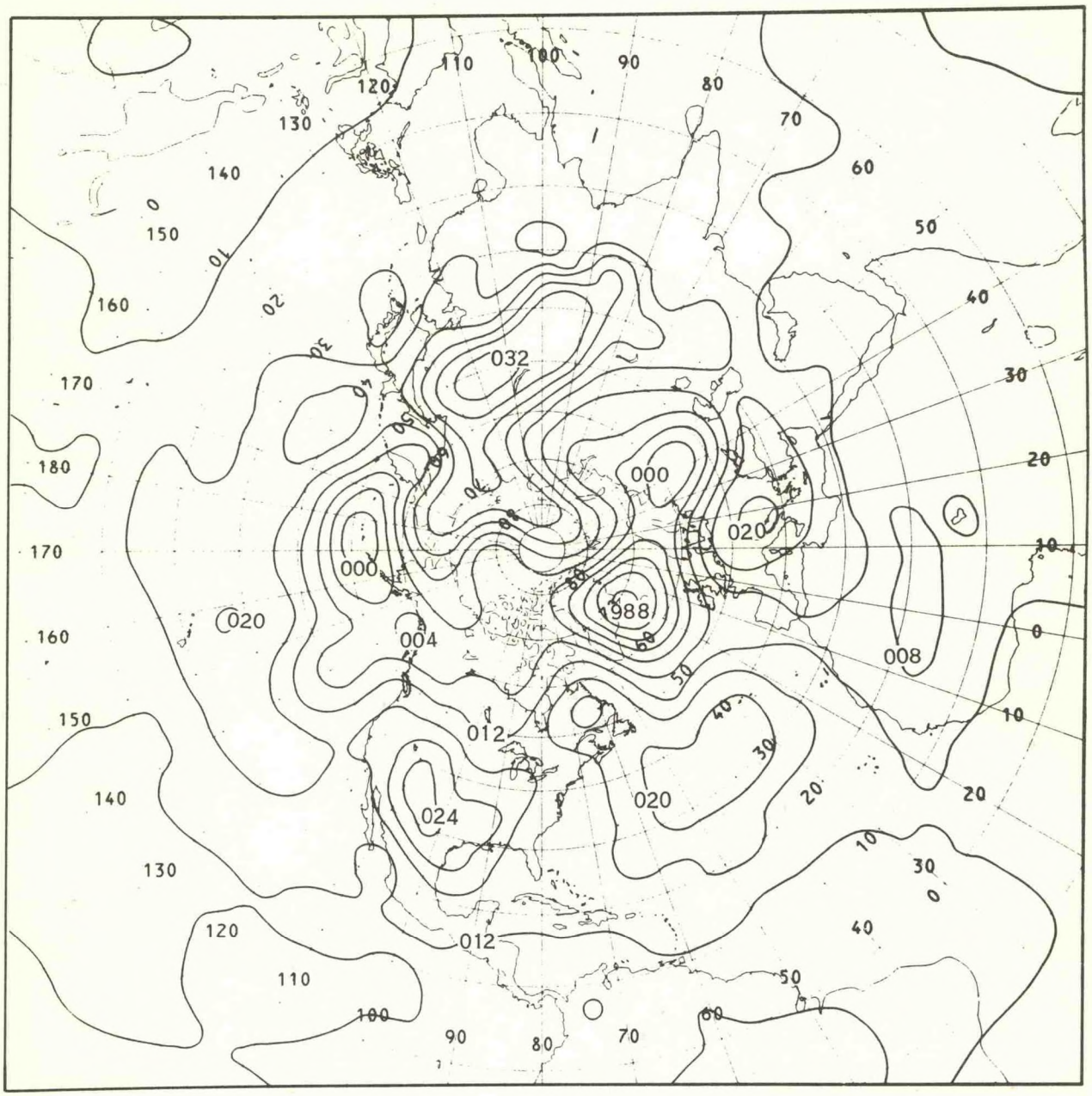

Figure 9.--E4 model, sea level pressure, 24 hr from 0000 GMT Oct. 8, 1976--contour interval 4 mb.

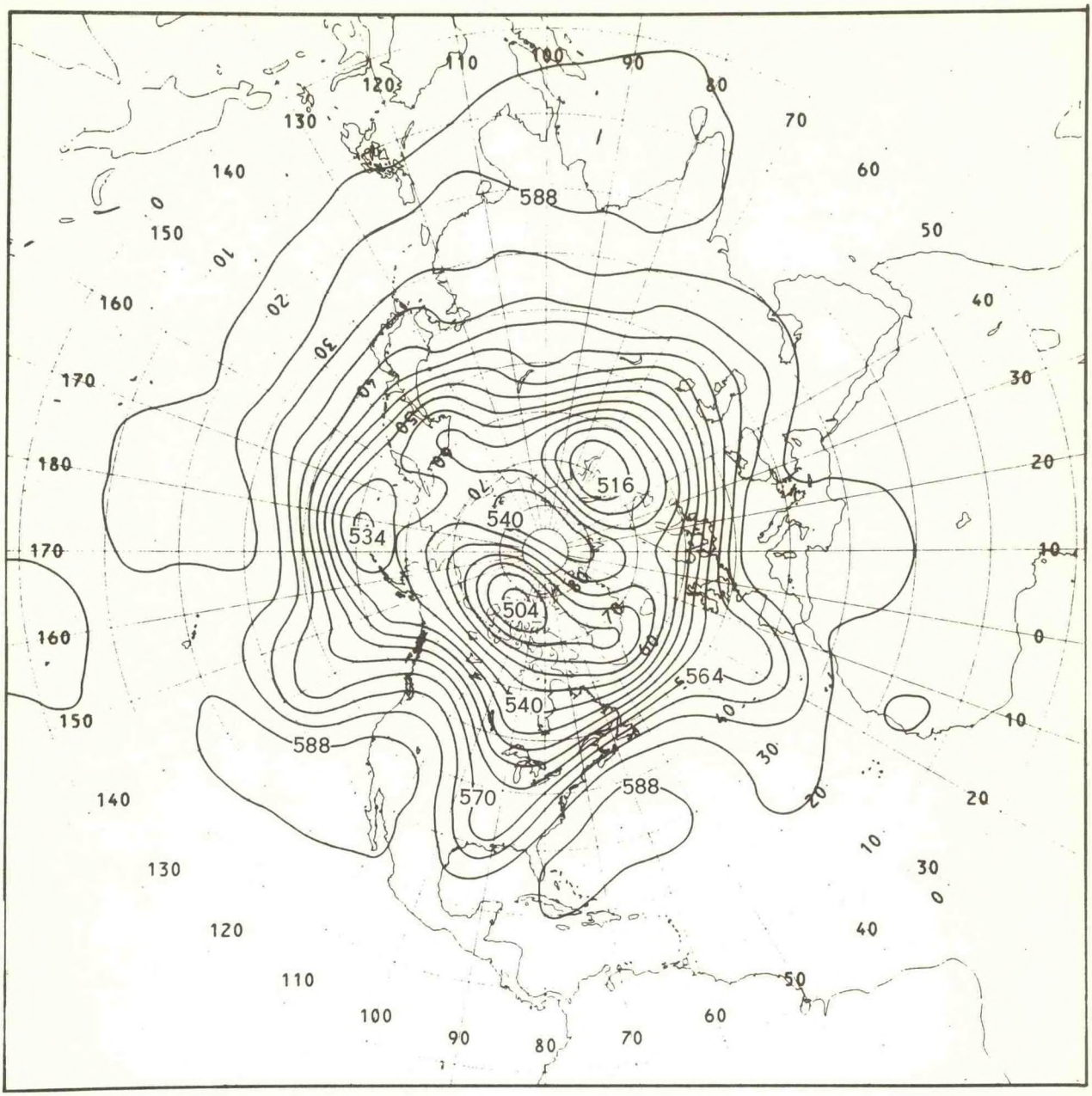

Figure 10.--E2 model, 500-mb heights, 24 hr from 0000 GMT Oct. 8, 1976--contour interval 6 decameters.

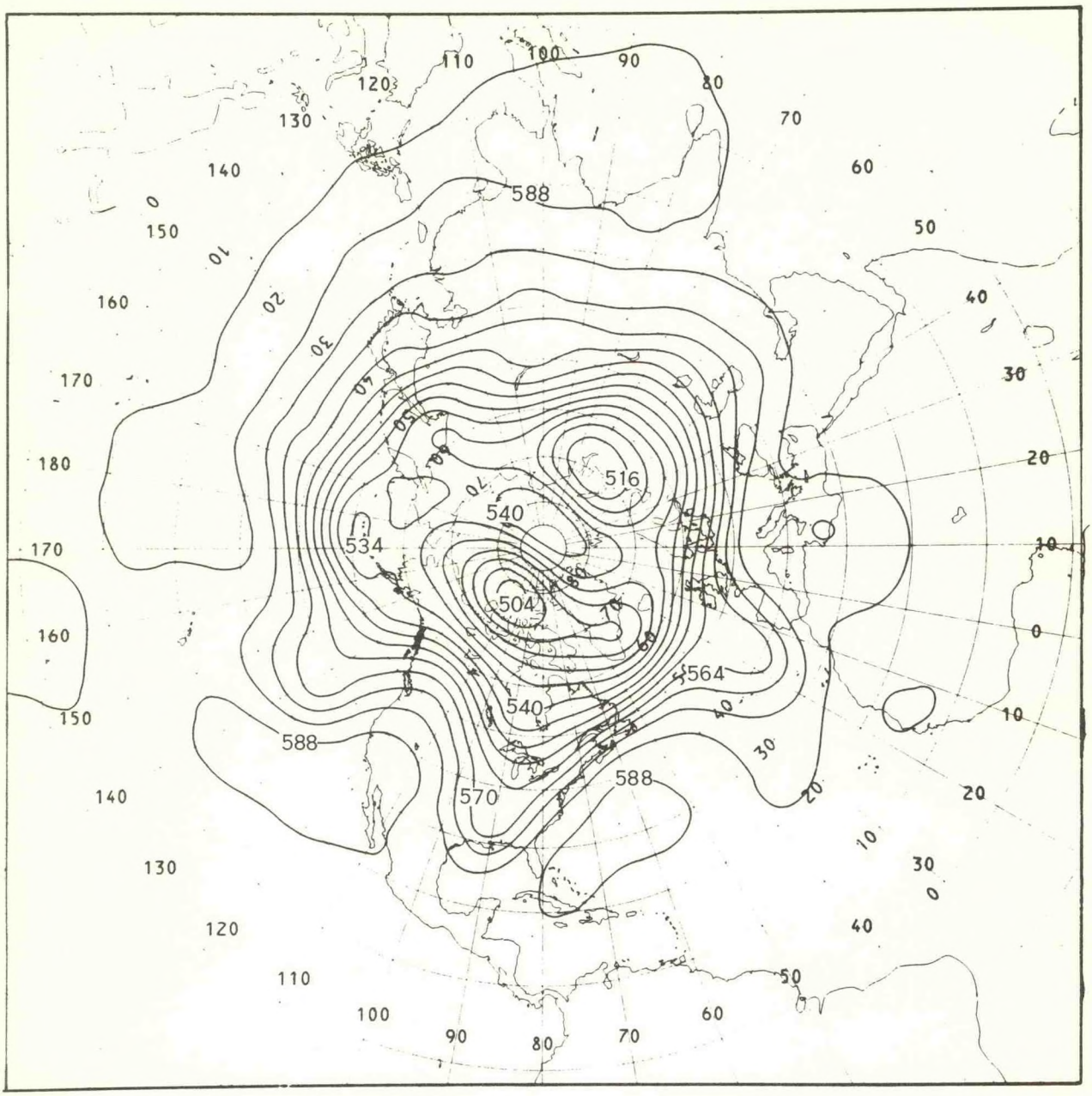

Figure 11.--E4 model, 500-mb heights, 24 hr from 0000 GMT Oct. 8, 1976--contour interval 6 decameters.

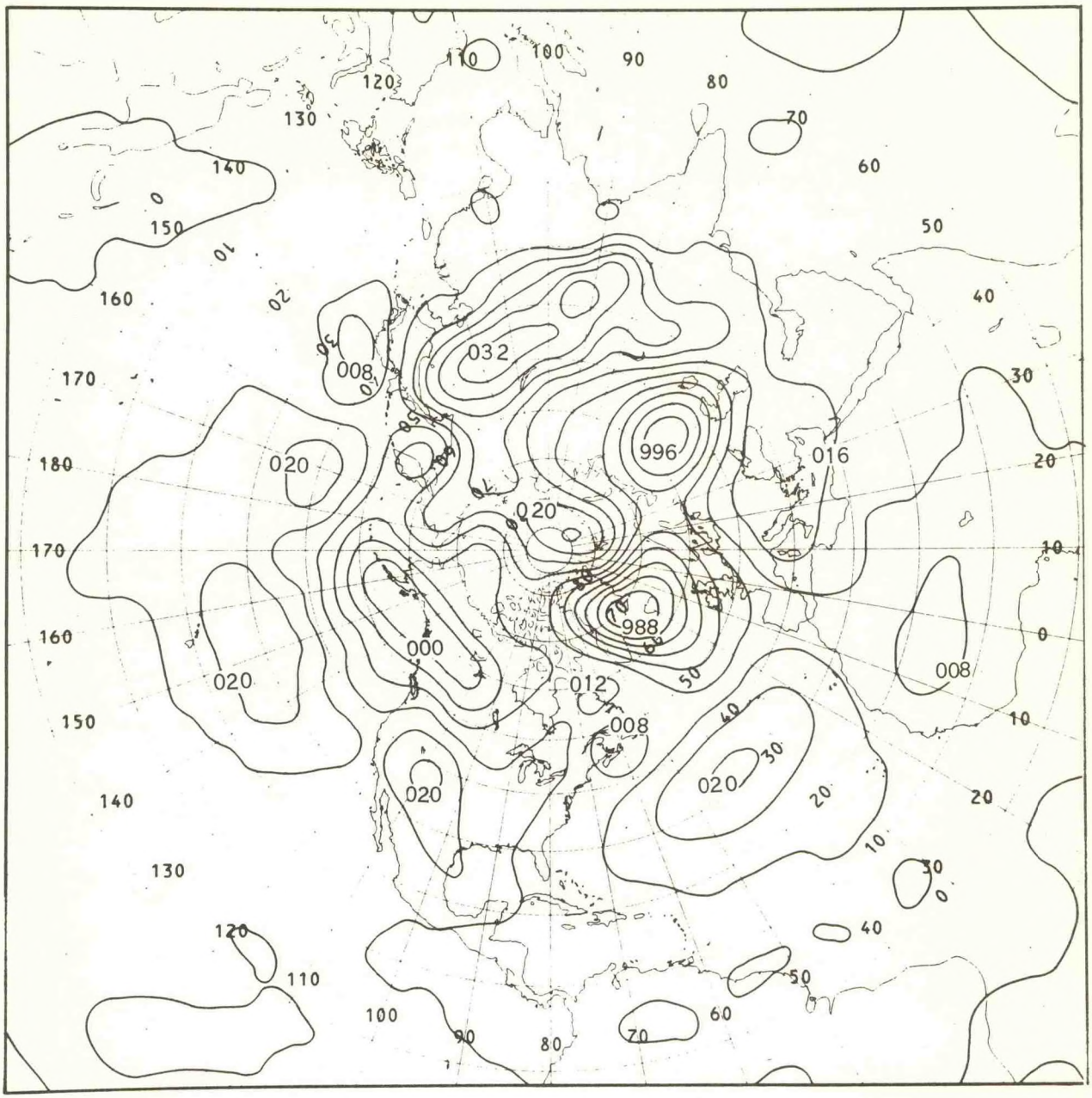

Figure 12.--E2 model, sea level pressure, 48 hr--contour interval 4 mb.

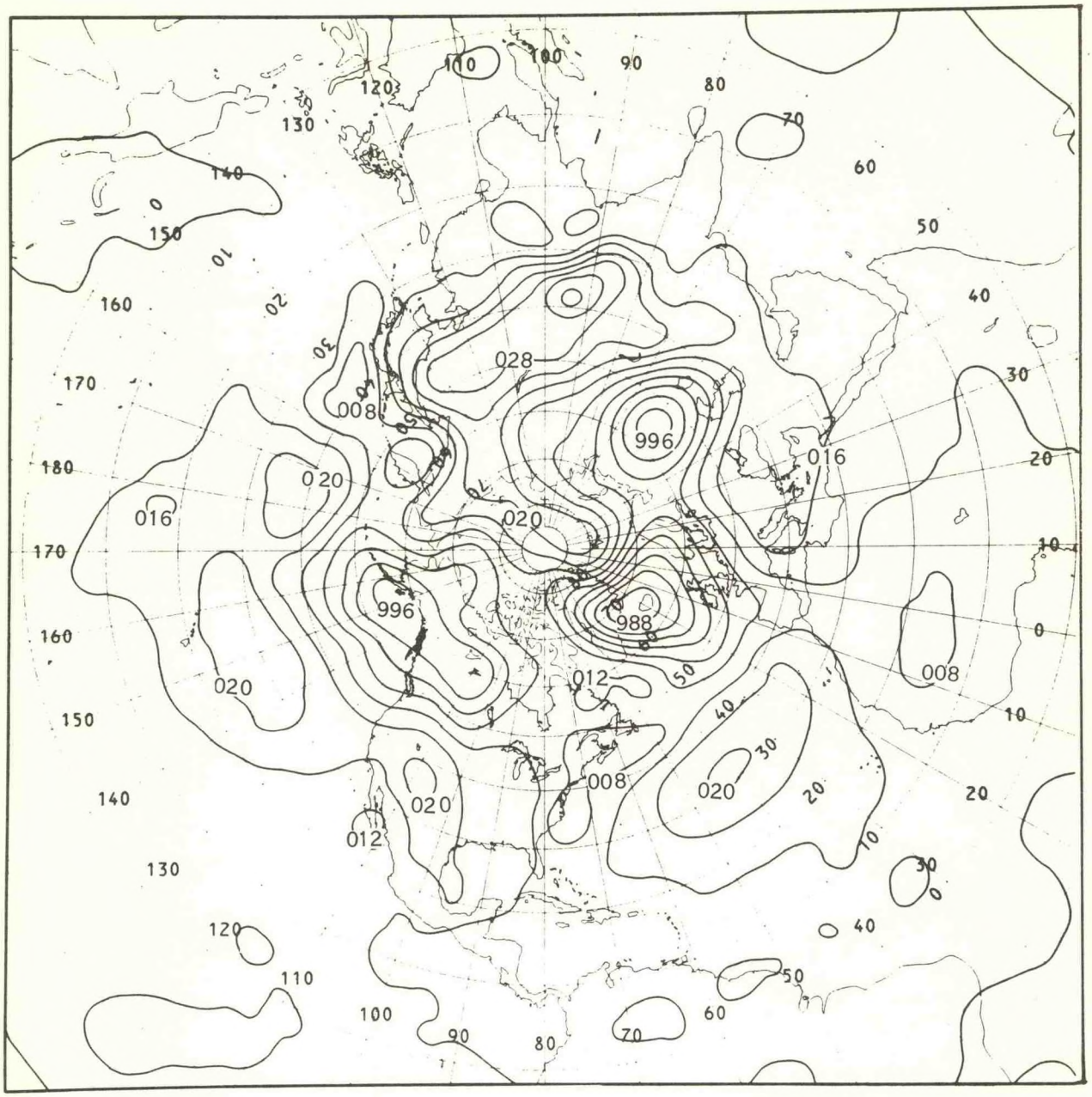

Figure 13.--E4 model, sea level pressure, 48 hr--contour interval 4 mb.

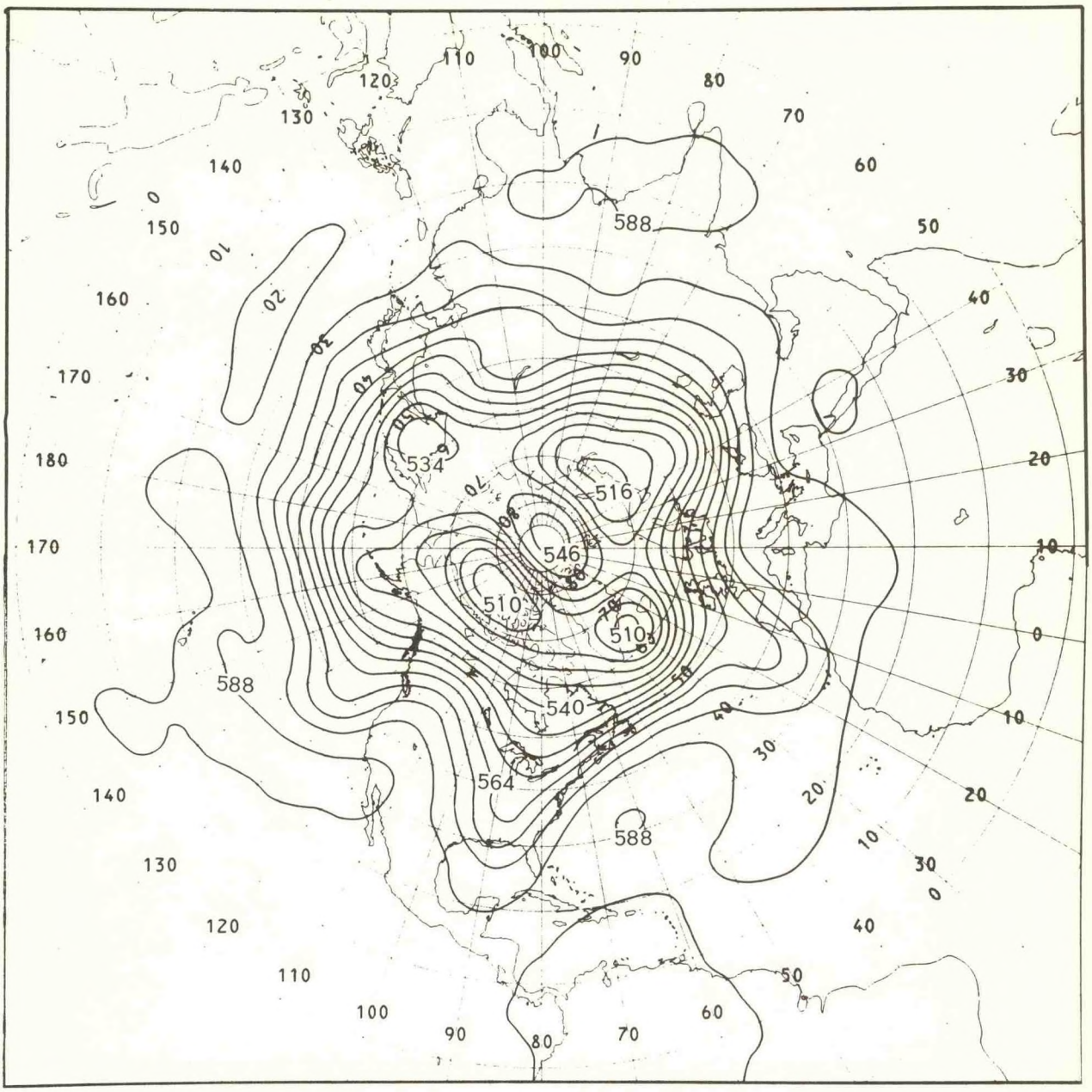

Figure 14.--E2 model, 500-mb heights, 48 hr--contour interval 6 decameters.

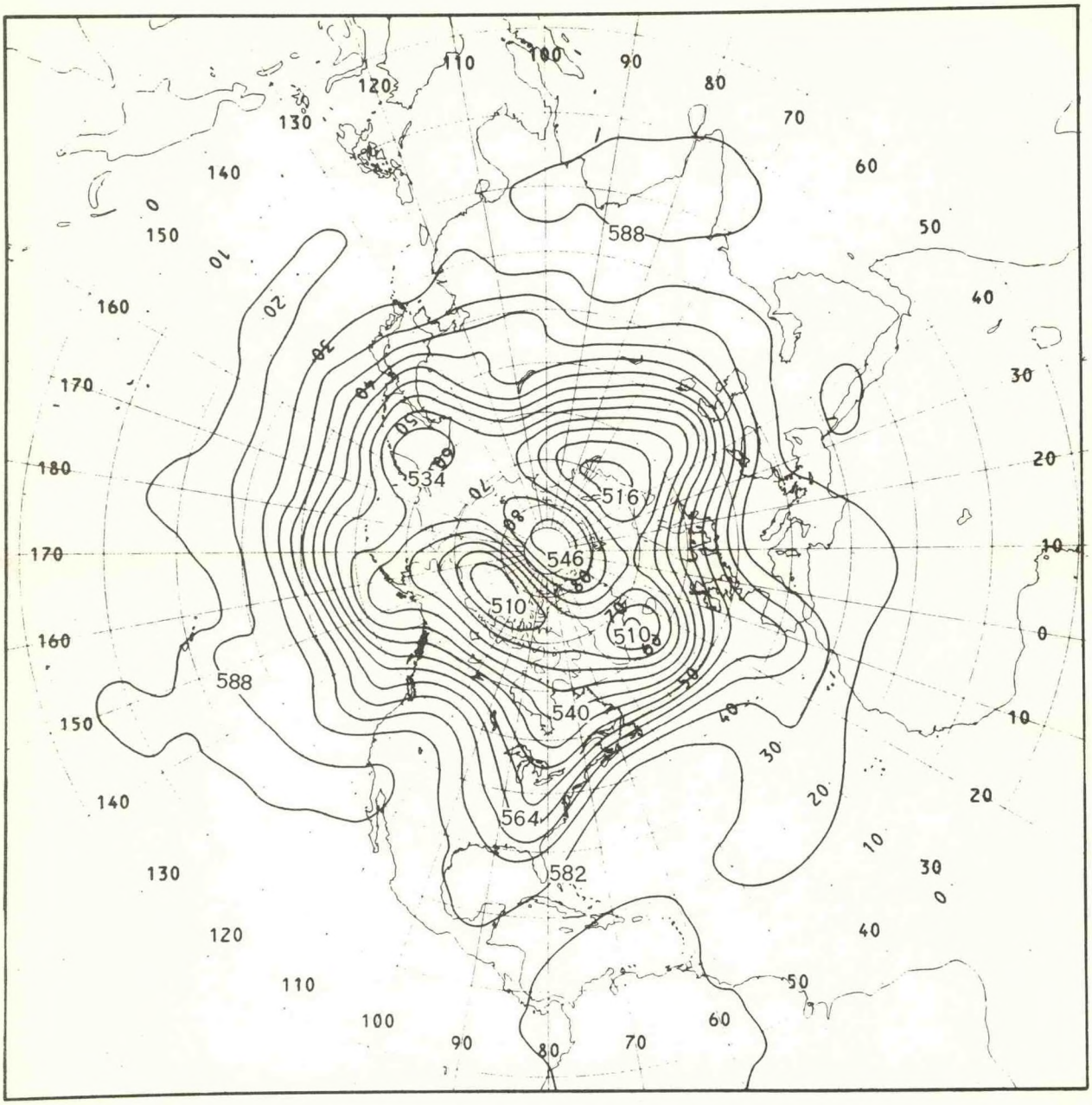

Figure 15.--E4 model, 500-mb heights, 48 hr--contour interval 6 decameters.

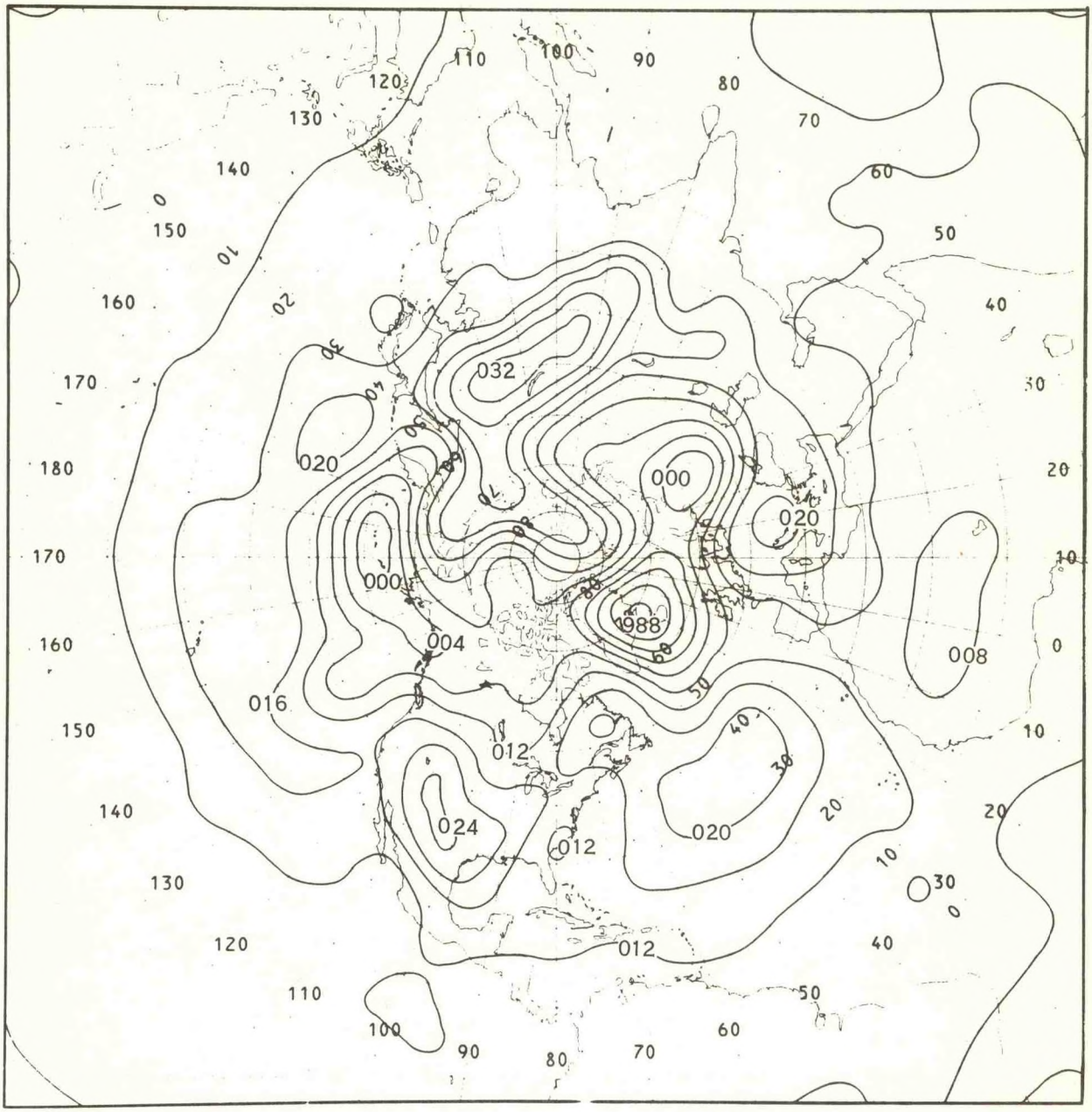

Figure 16.--S4 model, sea level pressure, 24 hr from 0000 GMT Oct. 8, 1976--contour interval 4 mb.

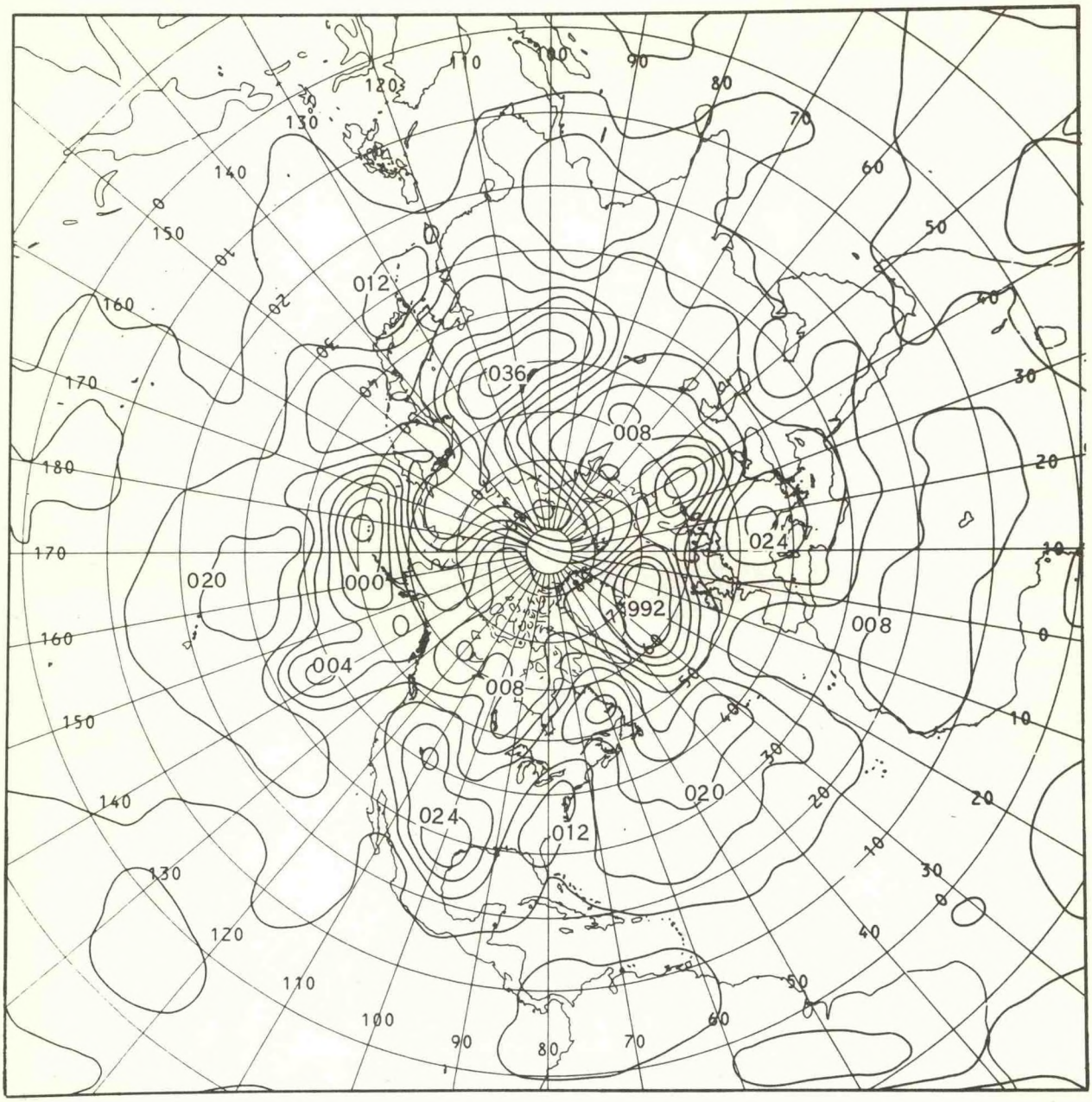

Figure 17.--6L PE model, sea level pressure, 24 hr from 0000 GMT Oct. 8,1976--contour interval 4 mb.

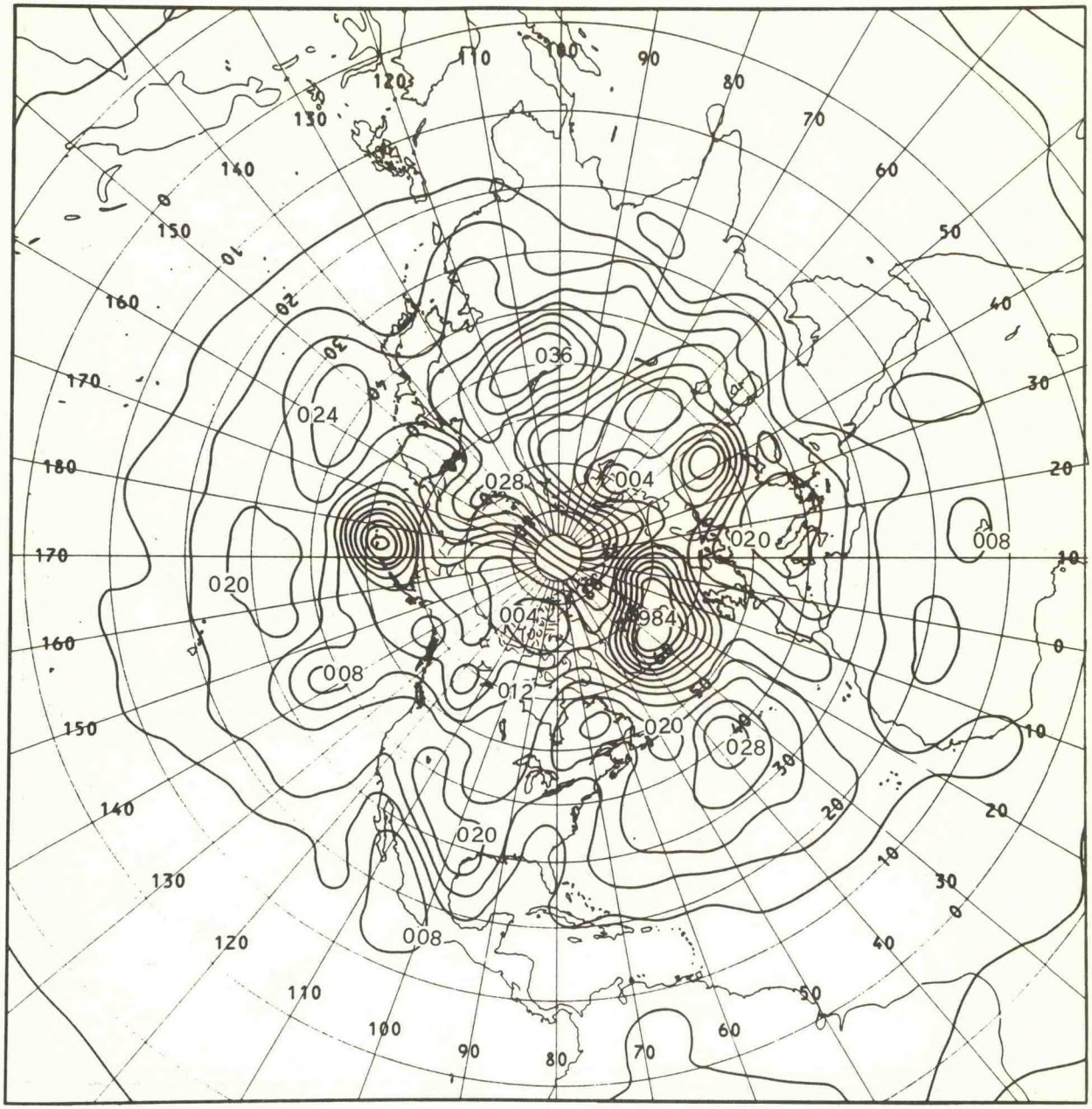

Figure 18.--NMC sea level pressure analysis, 0000 GMT Oct. 9, 1976, 24-hr verification--contour interval 6 decameters.

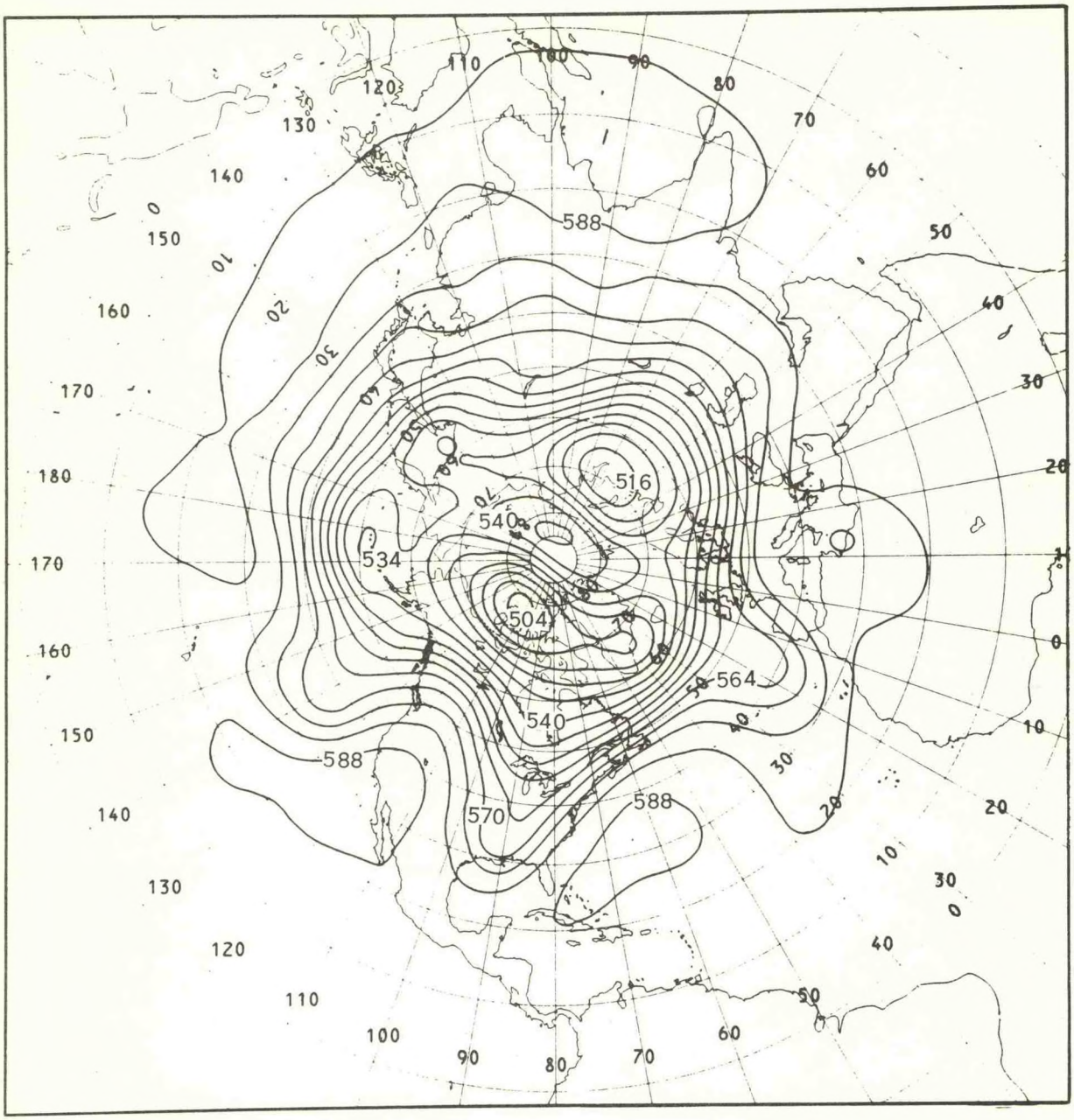

Figure 19.--S4 model, 500-mb height, 24 hr from 0000 GMT Oct. 8, 1976--contour interval 6 decameters.

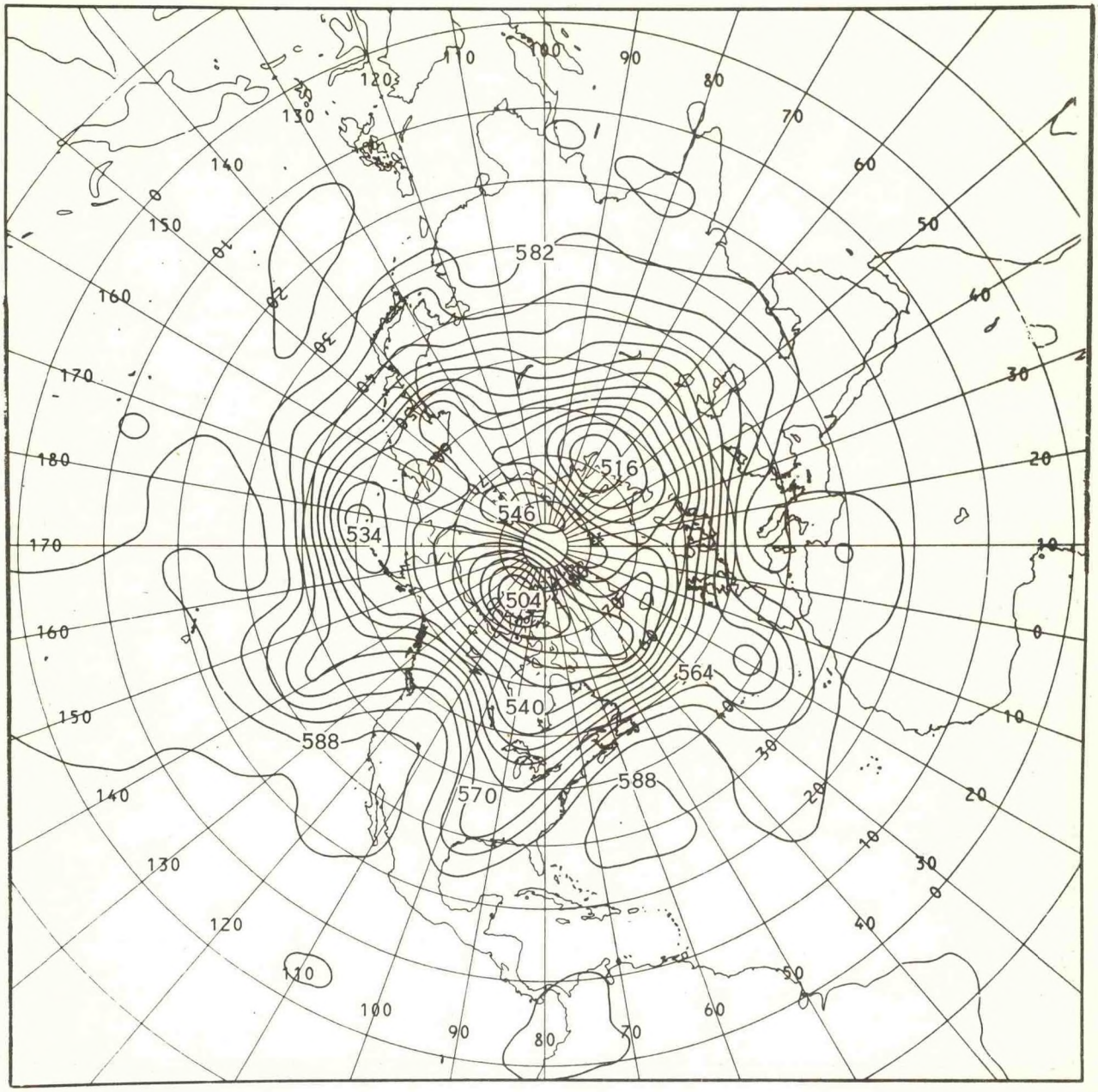

Figure 20.--6L PE model, 500-mb height, 24 hr from 0000 GMT Oct. 8, 1976--contour interval 6 decameters.

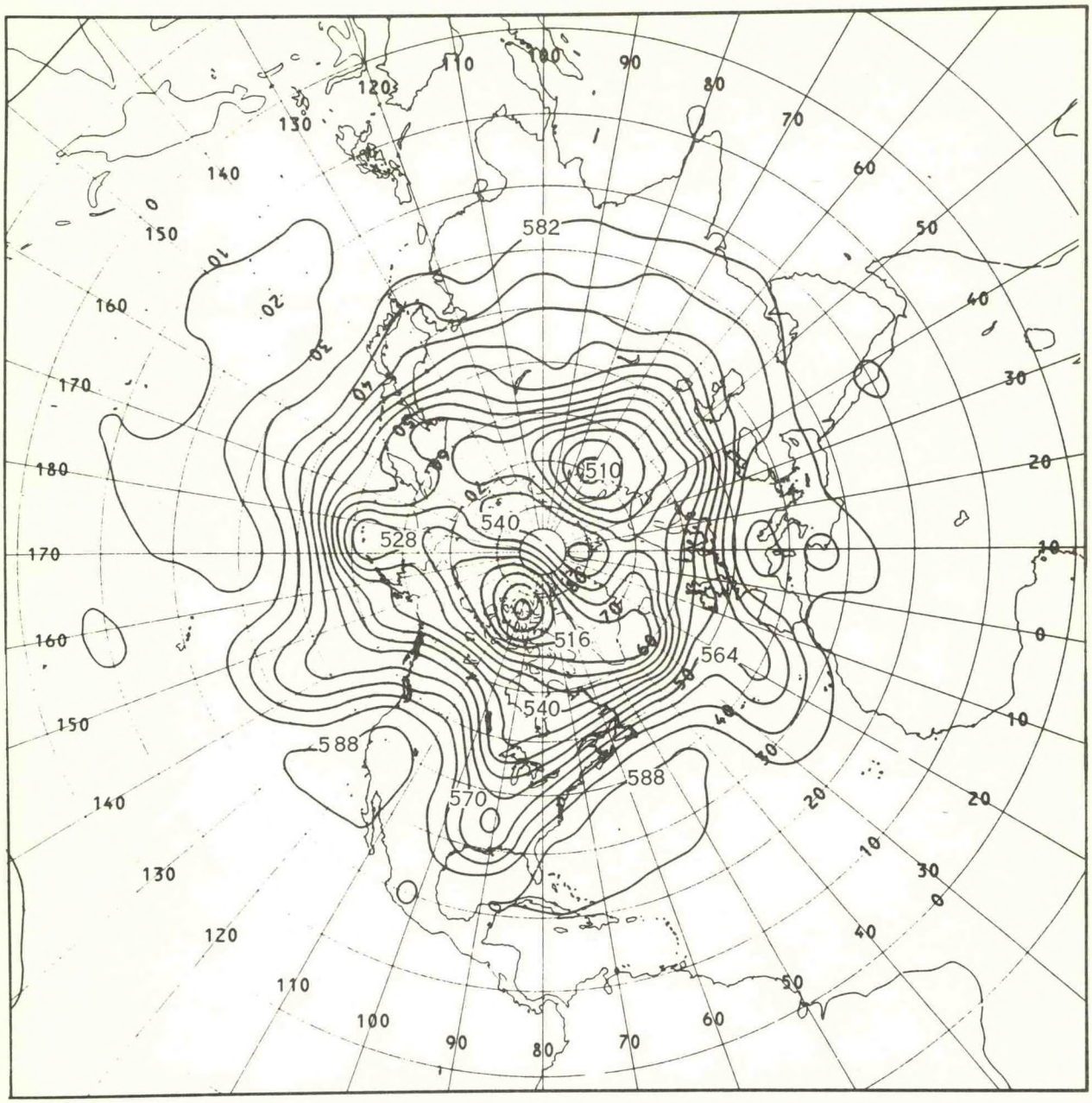

Figure 21.--NMC 500-mb height analysis, 0000 GMT Oct. 9, 1976, 24-hr verification--contour interval 6 decameters.

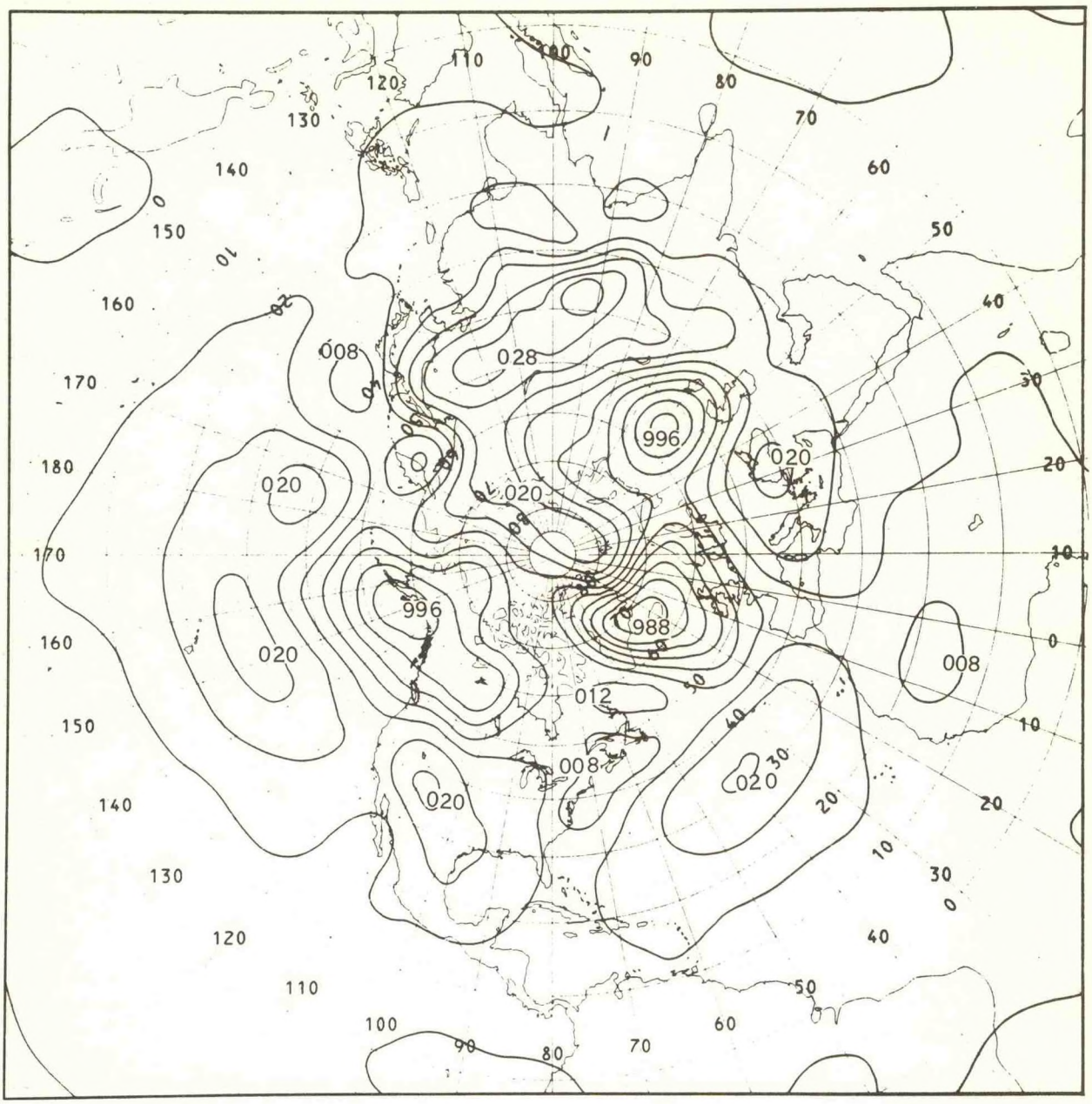

Figure 22.--S4 model, sea level pressure, 48 hr--contour interval 4 mb.

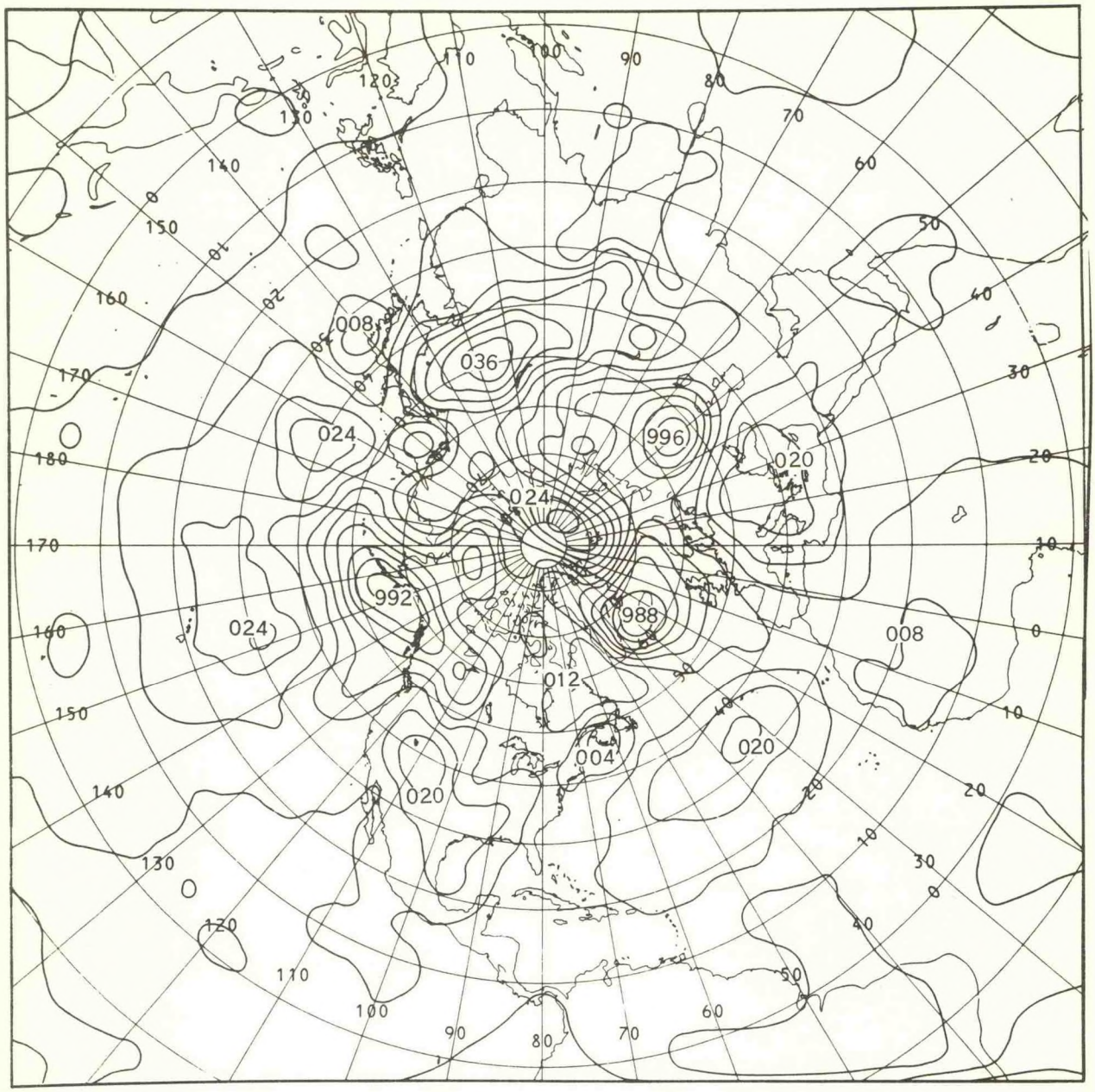

Figure 23.--6L PE model, sea level pressure, 48 hr--contour interval 4 mb.

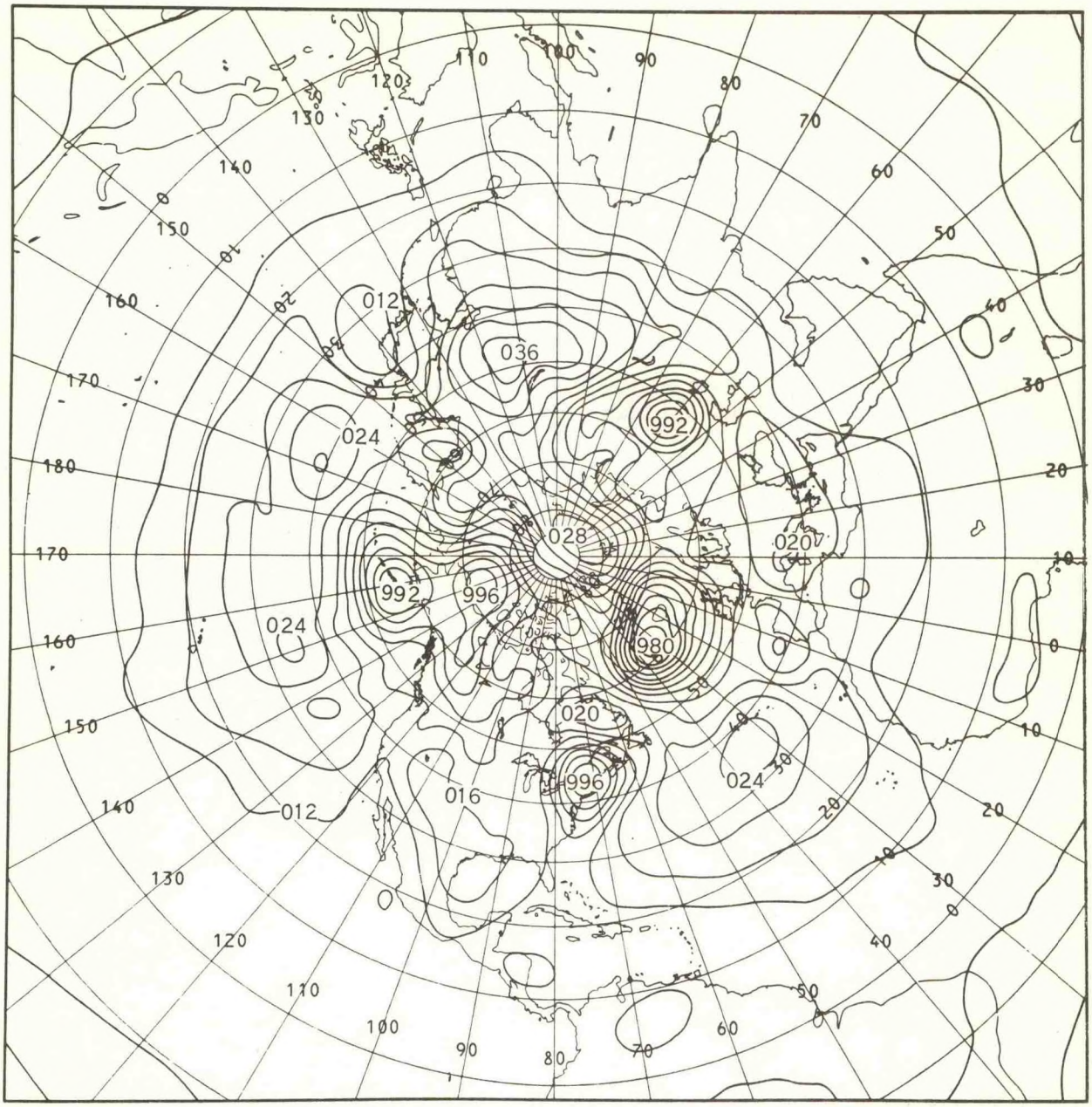

Figure 24.--NMC sea level pressure analysis, 0000 GMT Oct. 10, 1976, 48-hr verification--contour interval 4 mb.

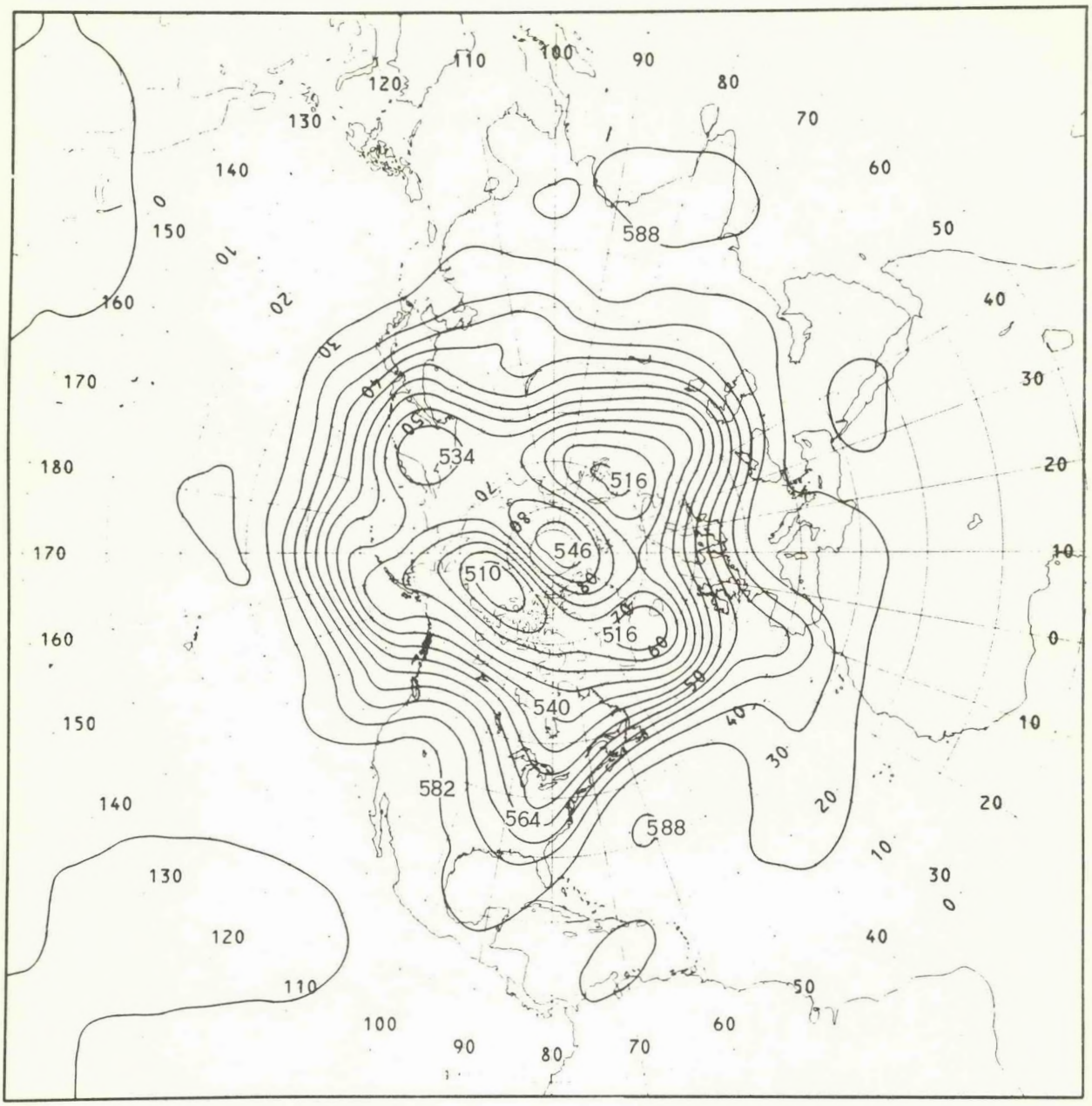

Figure 25.--S4 model, 500-mb height, 48 hr--contour interval 6 decameters.

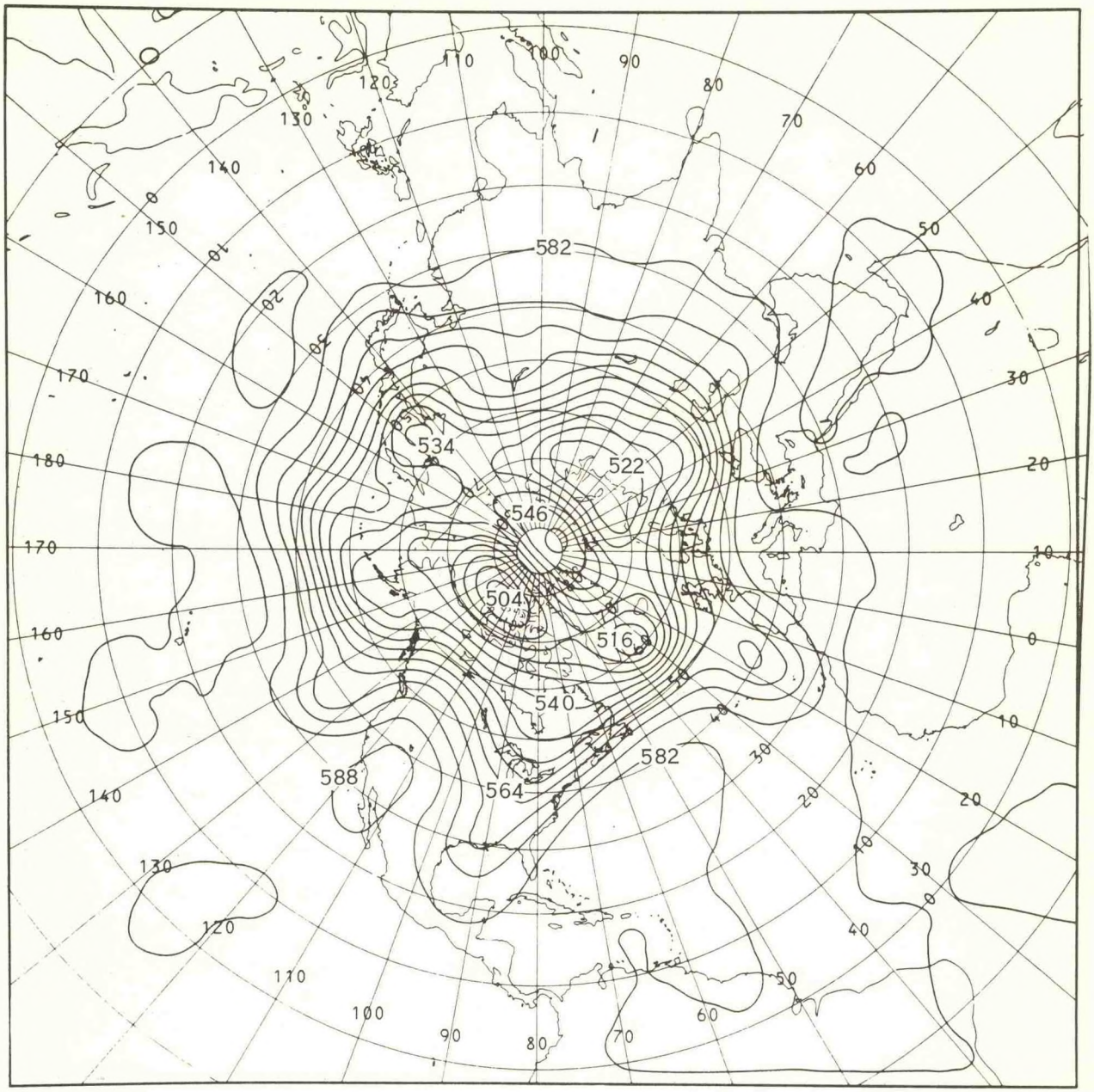

Figure 26.--6L PE model, 500-mb height, 48 hr--contour interval 6 decameters.

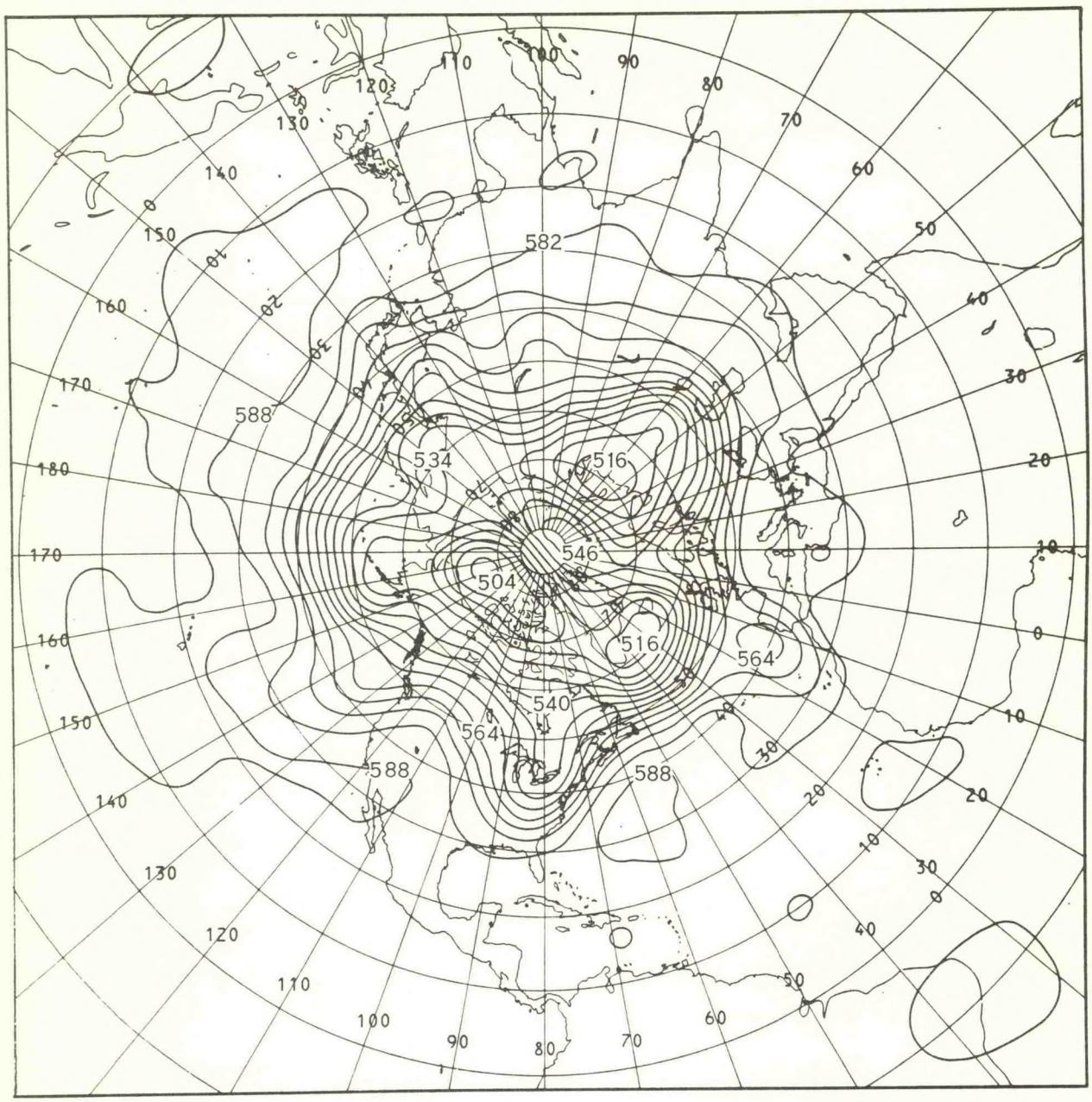

Figure 27.--NMC 500-mb height analysis, 0000 GMT Oct. 10, 1976, 48-hr verification--contour interval 6 decameters.

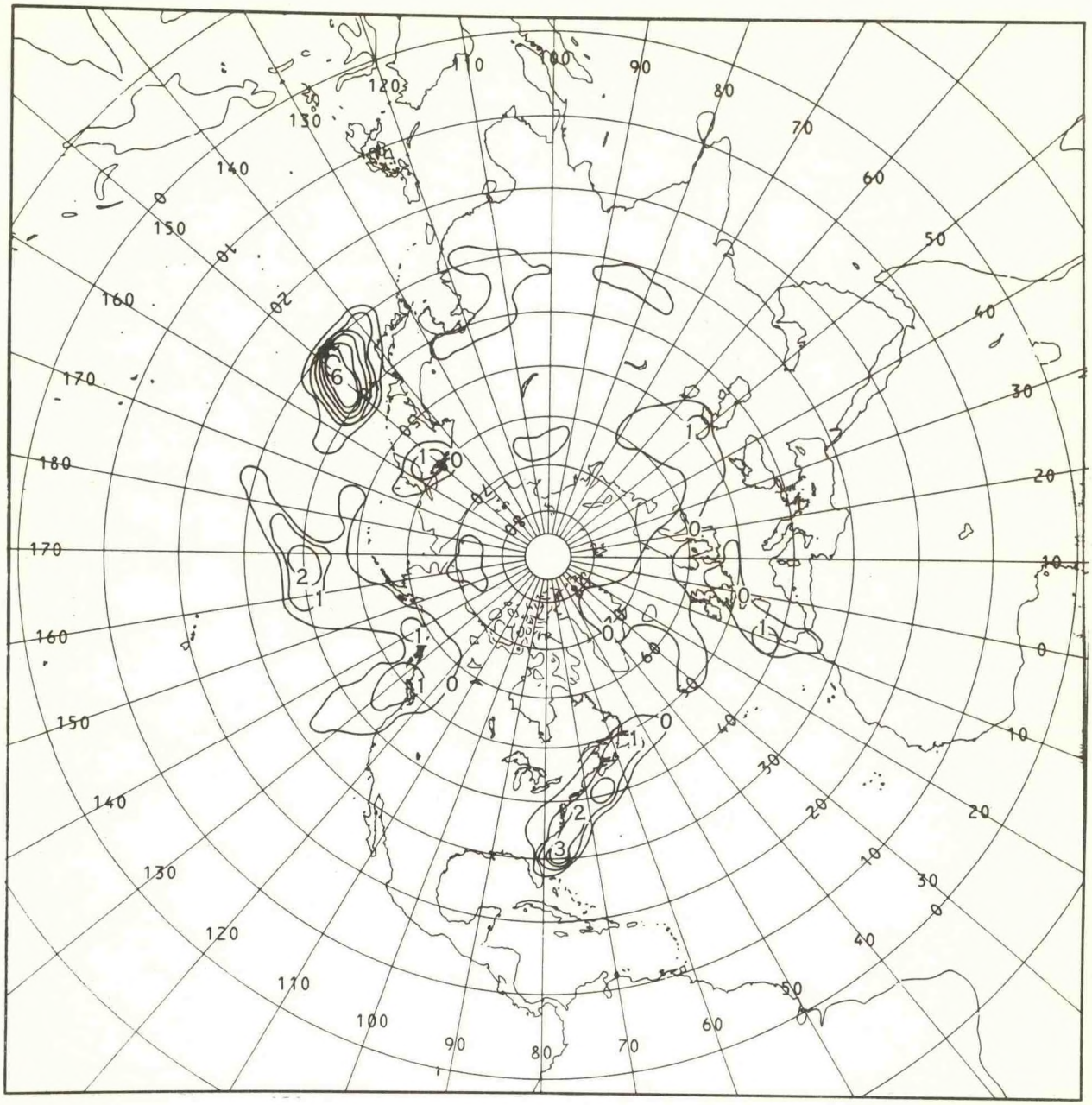

Figure 28.--E4 model, 36-48 hr accumulated precipitation from 0000 GMT Oct. 8, 1976--contour interval 1 centimeter.

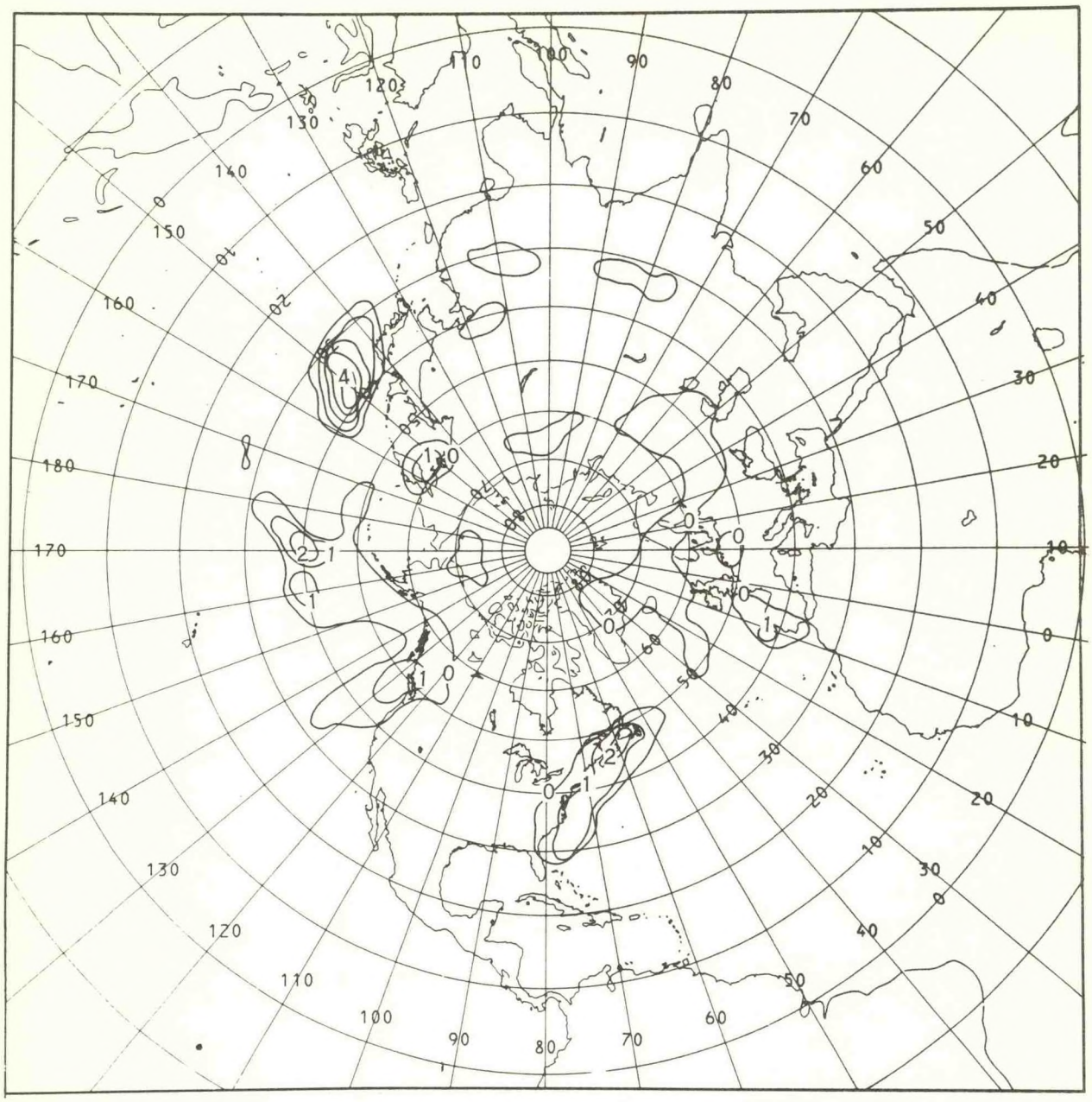

Figure 29.--S4 model, 36-48 hr accumulated precipitation from 0000 GMT Oct. 8, 1976--contour interval 1 centimeter.

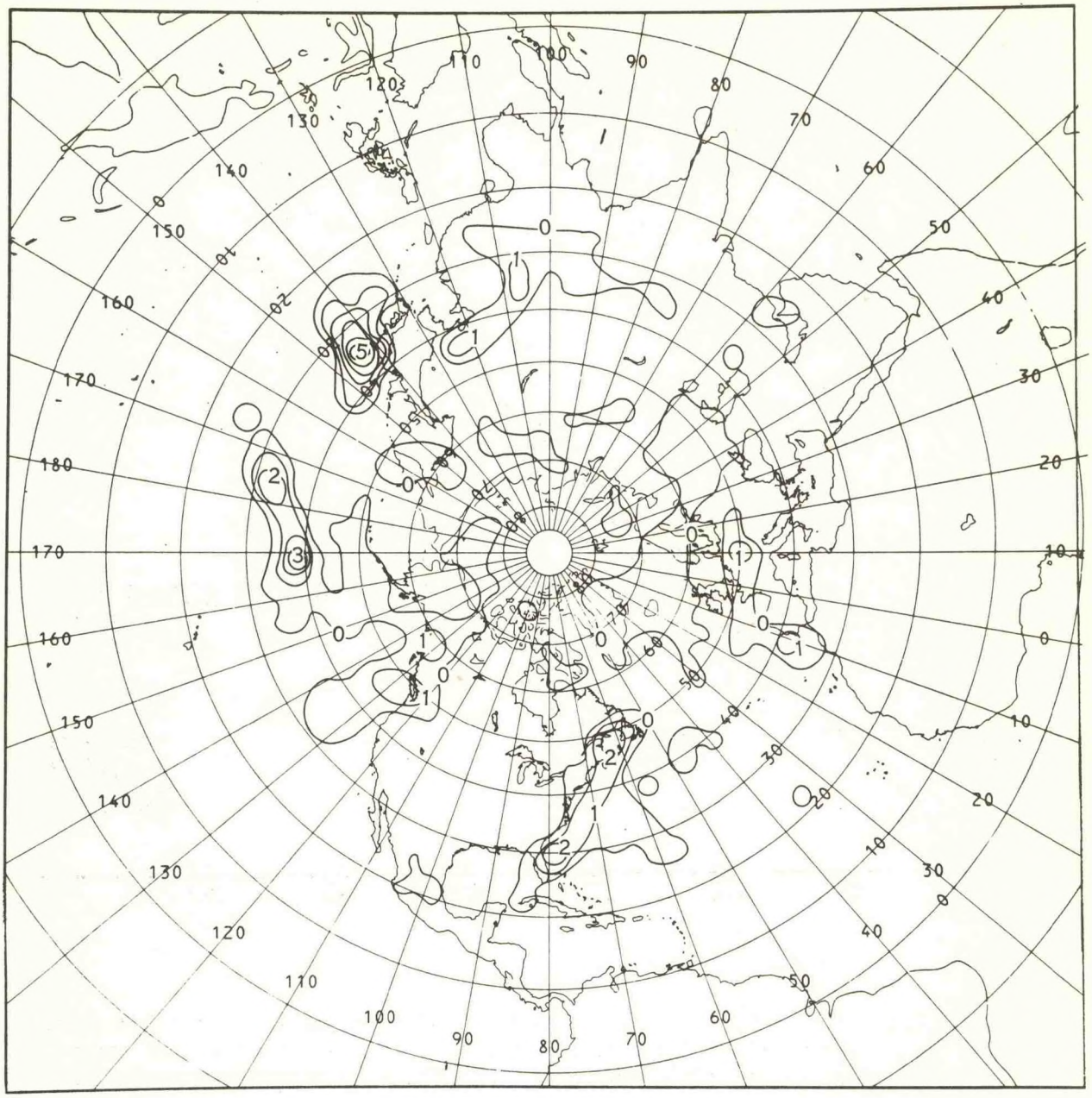

Figure 30.-- 6L PE model, 36-48 hr accumulated precipitation from 0000 GMT Oct. 8, 1976-- contour interval 1 centimeter.

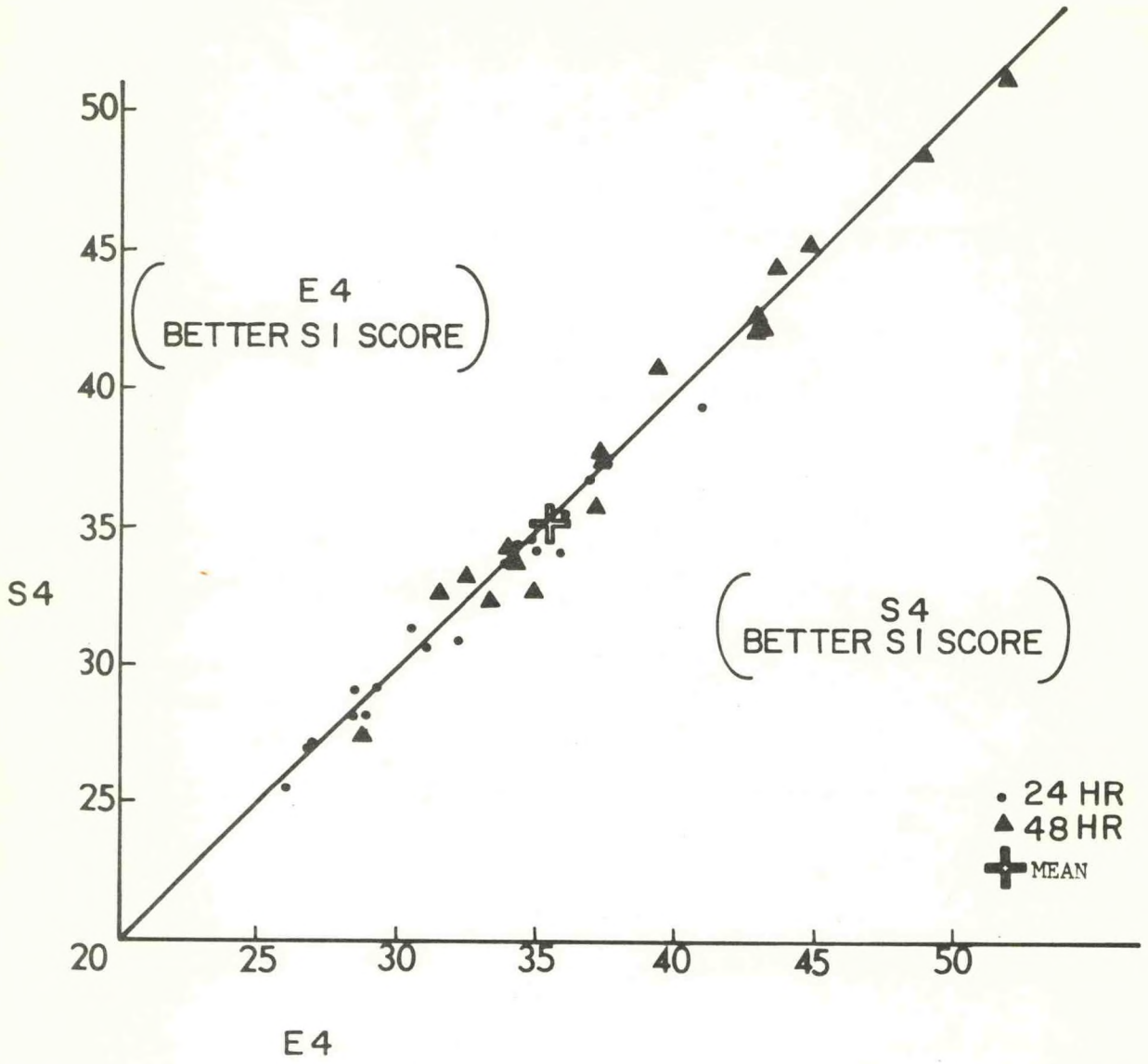

Figure 3.--E4 and S4 models S1 scores (500 mb) at 24 hr and 48 hr for 6 cases in October 1976. Each data point is from one of three NMC verification areas in the Northern Hemisphere (North America, Europe, and Asia).

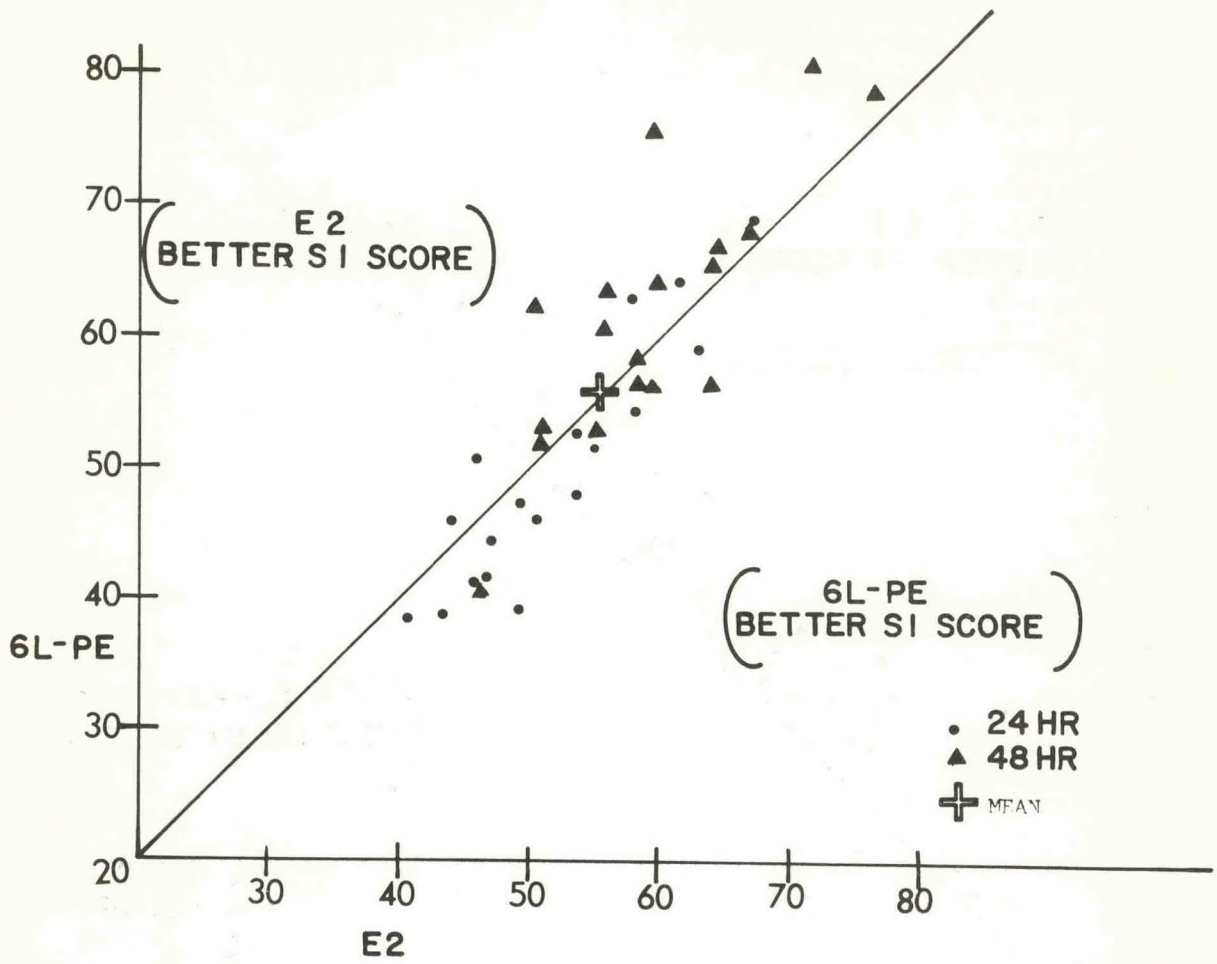

Figure 32.--6L PE and E2 models S1 scores (sea level pressure) at 24 hr and 48 hr for 6 cases in October 1976.

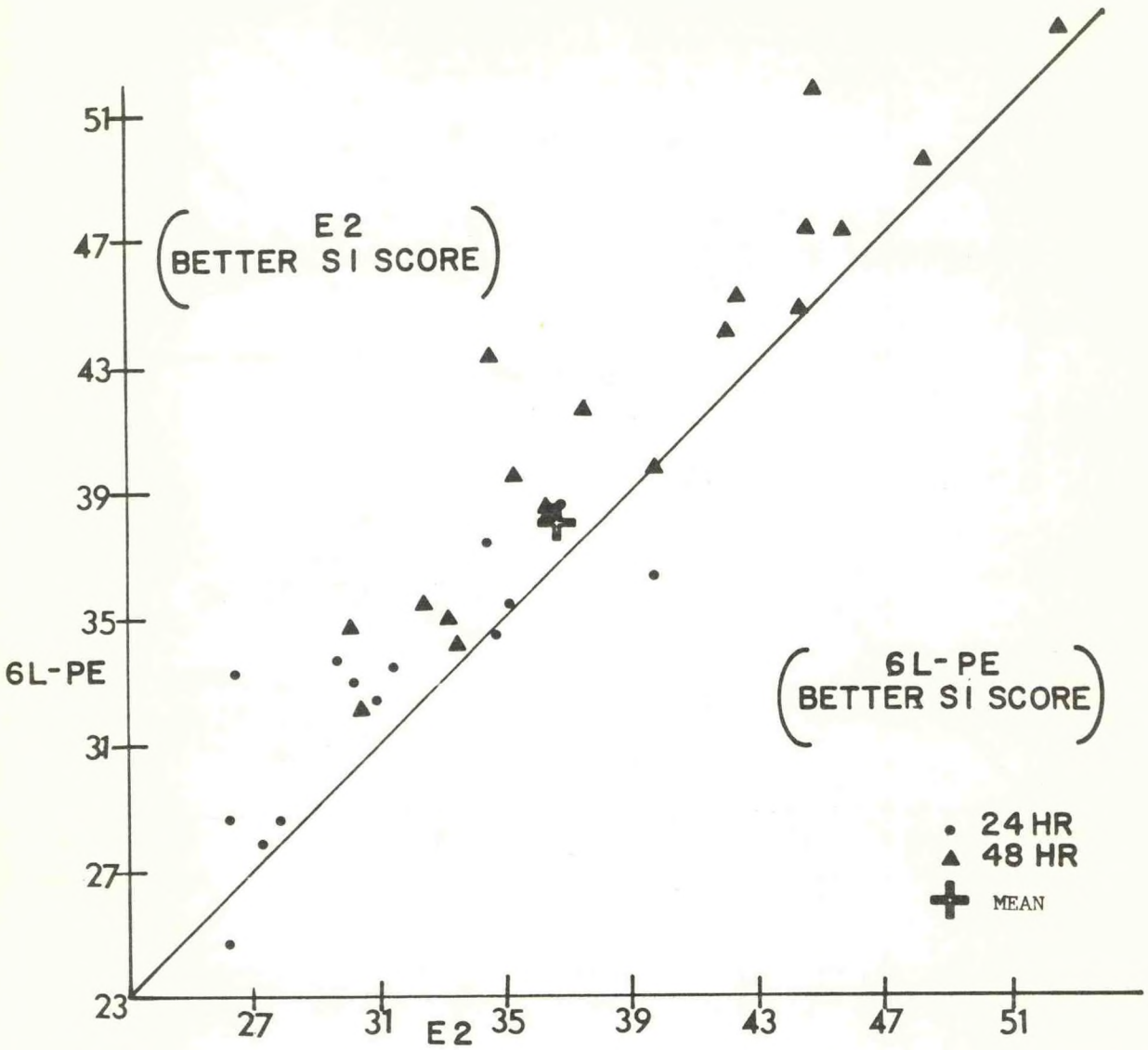

Figure 33.--6L PE and E2 models S1 scores (500 mb) at 24 hr and 48 hr for 6 cases in October 1976.

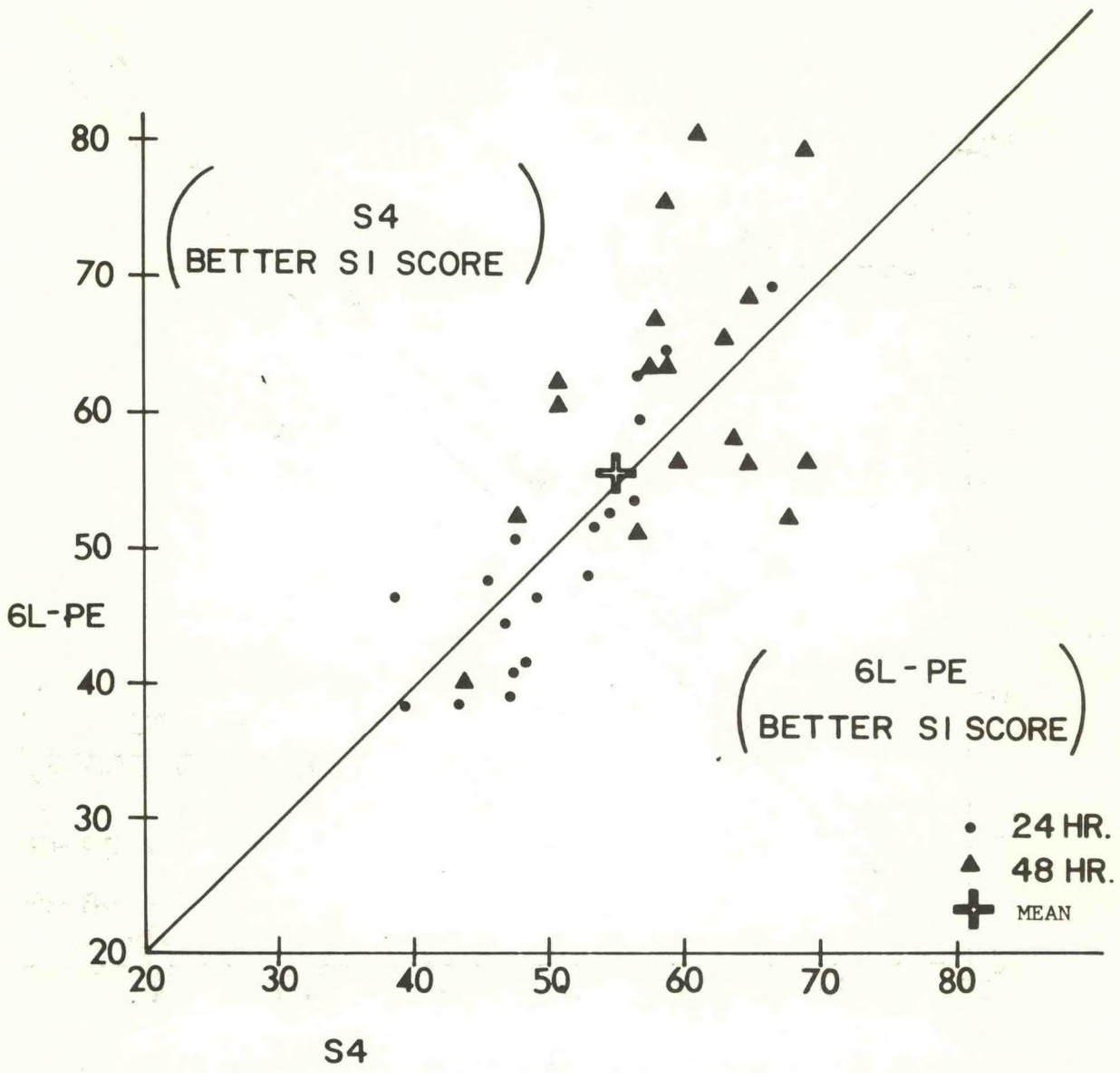

Figure 34.--6L PE and S4 models S1 scores (sea level pressure) at 24 hr and 48 hr for 6 cases in October 1976.

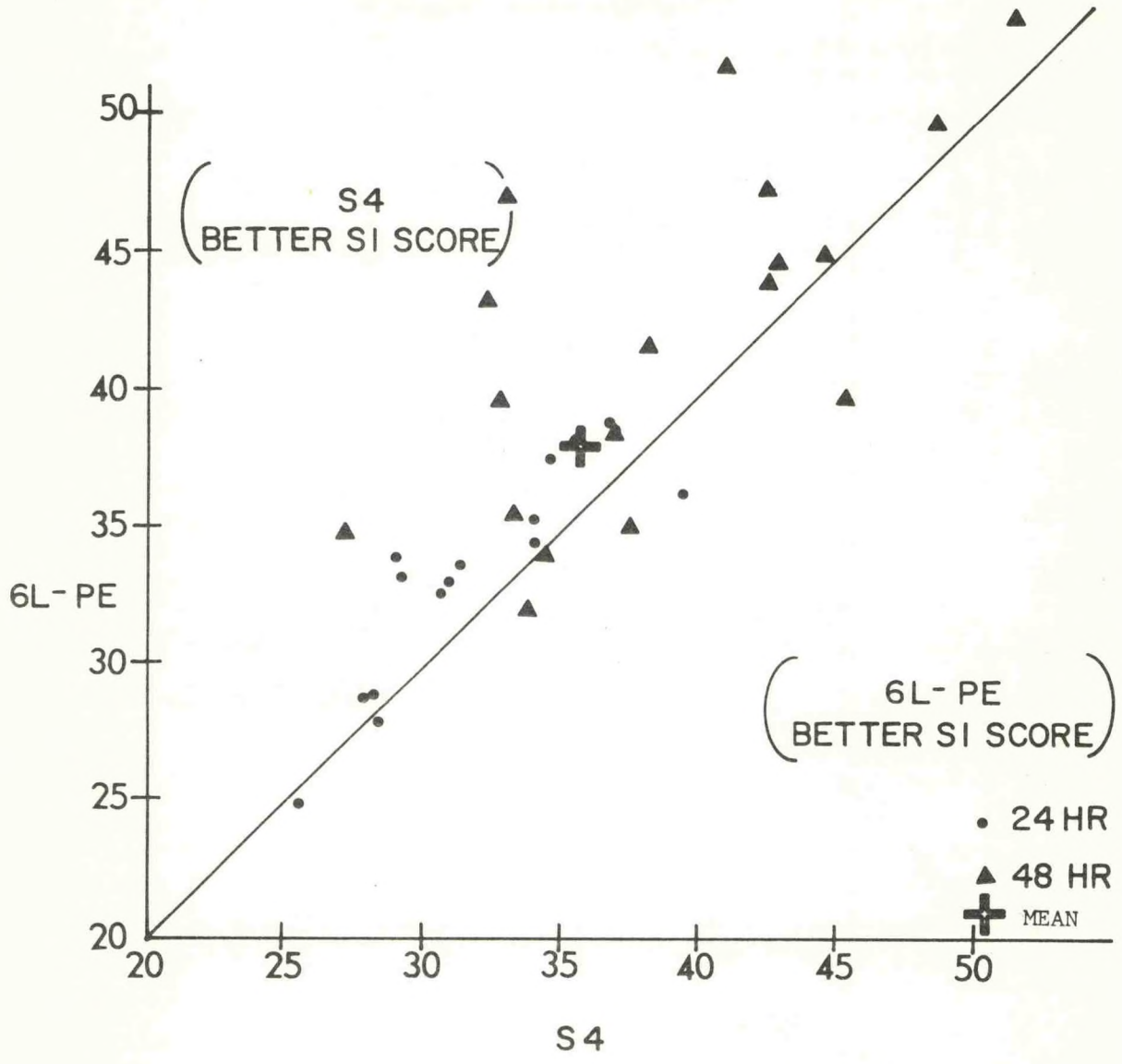

Figure 35.--6L PE and S4 models S1 scores (500 mb) at 24 hr and 48 hr for 6 cases in October 1976.

(Continued from inside front cover)

NOAA Technical Memorandums

NWS NMC 49 A Study of Non-Linear Computational Instability for a Two-Dimensional Model. Paul D. Polger, February 1971. (COM-71-00246)

NWS NMC 50 Recent Research in Numerical Methods at the National Meteorological Center. Ronald D. McPherson, April 1971. (COM-71-00595)

NWS NMC 51 Updating Asynoptic Data for Use in Objective Analysis. Armand J. Desmarais, December 1972. (COM-73-10078)

NWS NMC 52 Toward Developing a Quality Control System for Rawinsonde Reports. Frederick G. Finger and Arthur R. Thomas, February 1973. (COM-73-10673)

NWS NMC 53 A Semi-Implicit Version of the Shuman-Hovermale Model. Joseph P. Gerrity, Jr., Ronald D. McPherson, and Stephen Scolnik. July 1973. (COM-73-11323)

NWS NMC 54 Status Report on a Semi-Implicit Version of the Shuman-Hovermale Model. Kenneth Campana, March 1974. (COM-74-11096/AS)

NWS NMC 55 An Evaluation of the National Meteorological Center's Experimental Boundary Layer model. Paul D. Polger, December 1974. (COM-75-10267/AS)

NWS NMC 56 Theoretical and Experimental Comparison of Selected Time Integration Methods Applied to Four-Dimensional Data Assimilation. Ronald D. McPherson and Robert E. Kistler, April 1975. (COM-75-10882/AS)

NWS NMC 57 A Test of the Impact of NOAA-2 VTPR Soundings on Operational Analyses and Forecasts. William D. Bonner, Paul L. Lemar, Robert J. Van Haaren, Armand J. Desmarais, and Hugh M. O'Neil, February 1976. (PB-256075)

NWS NMC 58 Operational-Type Analyses Derived Without Radiosonde Data from NIMBUS 5 and NOAA 2 Temperature Soundings. William D. Bonner, Robert van Haaren, and Christopher M. Hayden, March 1976. (PB-256099)

NWS NMC 59 Decomposition of a Wind Field on the Sphere. Clifford H. Dey and John A. Brown, Jr. April 1976. (PB-265422)

NWS NMC 60 The LFM Model 1976: A Documentation. Joseph P. Gerrity, Jr., December 1977.